

OPTIMIZE VENTILATION SYSTEMS IN CONFINED WORKPLACES USING  
COMPUTATIONAL FLUID DYNAMICS

A Thesis

by

ZEREN JIAO

Submitted to the Office of Graduate and Professional Studies of  
Texas A&M University  
in partial fulfillment of the requirements for the degree of

MASTER OF SCIENCE

Chair of Committee,	M. Sam Mannan
Committee Members,	Mahmoud M. El-Halwagi Eric L. Petersen
Head of Department,	M. Nazmul Karim

May 2018

Major Subject: Chemical Engineering

Copyright 2018 Zeren Jiao

## ABSTRACT

Chemical industry and society always want to eliminate the damage to the environment and lower the casualty if an incident occurs. Finding a more efficient and effective way to achieve this goal is now more critical than ever. The ventilation system is the most common engineering method to control the airborne toxic and explosive material in confined workplaces. The purpose of ventilation is to dilute or remove the toxic and explosive vapors with air to prevent potential poisoning or explosion.

Optimized ventilation system design is critical to industrial hygiene control and to improve ventilation system efficiency. Insufficient ventilation can directly threaten the worker's health and life. A properly designed industrial ventilation system can significantly improve the safety of workplaces and maintain a comfortable work condition. Ventilation can also prevent the corrosion and increase the life of process units and equipment. Newly designed chemical facilities should make sure that proper ventilation systems are used to control air quality, and plants already in operation should also carefully evaluate the work environment to ensure compliance with the federal codes and regulations.

Computational Fluid Dynamics has been used in this thesis to analyze the fluid dynamics performance in the laboratory environment using the dilution ventilation system. A variety of different ventilation system installation schemes are proposed, and the performance of different schemes is examined and compared through simulation to get the optimal installation plan for the best contaminant control.

The proposed scheme also optimizes the ventilating system installation by investigating the system's performance with different transmitted mediums. The results of

this work can serve as references to maximize the ventilation efficiency and minimize the energy cost.

## DEDICATION

This thesis is dedicated to my beloved  
parents, grandparents,  
all friends of mine,  
and  
my dear Hanyu

## ACKNOWLEDGEMENTS

I would like to thank my committee chair and academic advisor, Dr. M. Sam Mannan, for his constant support and insightful advice on my whole graduate career. He gave me the chance to join the Mary Kay O'Connor Process Safety Center, which is the best place for process safety study. I also would like to express gratitude to my committee members, Dr. Mahmoud M. El-Halwagi and Dr. Eric L. Peterson for their patient guidance and innovative ideas for my research. My research cannot be successfully done without their help and support.

Moreover, I also would like to thank my team leader Dr. Monir Ahammad for his continuous effort and careful guidance. All of my colleagues in the Mary Kay O'Connor Process Safety Center are like family for me; I can always learn from someone, and all of them are kind and warm-hearted.

Finally, I want to thank my mother and father, Luyi Gu and Zhen Jiao, my grandparents Zuyong Gu and Zhengyan Wang for their unconditional love and encouragement. I also want to thank my girlfriend Hanyu Xu for her love and support and wish you can be successfully admitted to PhD program in Texas A&M.

## CONTRIBUTORS AND FUNDING SOURCES

### **Contributors**

This work was supervised by a thesis committee consisting of Professor M. Sam Mannan and Professor Mahmoud M. El-Halwagi of the Department of Chemical Engineering and Professor Eric L. Petersen of the Department of Mechanical Engineering.

All work for the thesis was completed independently by the student.

### **Funding Sources**

There are no outside funding contributions to acknowledge related to the research and compilation of this document.

## TABLE OF CONTENTS

	Page
ABSTRACT.....	ii
DEDICATION.....	iv
ACKNOWLEDGEMENTS.....	v
CONTRIBUTORS AND FUNDING SOURCES.....	vi
LIST OF FIGURES.....	ix
LIST OF TABLES.....	xi
1. INTRODUCTION.....	1
1.1 Background and Motivation.....	1
1.2 Industrial Ventilation System.....	3
1.3 Computational Fluid Dynamics.....	6
1.4 Research Objectives.....	6
1.5 Outline of Research.....	7
2. LITERATURE REVIEW.....	9
2.1 Industrial Ventilation Systems.....	9
2.2 Assessment of Ventilation Systems.....	12
2.3 Simulation and Computational Techniques for Ventilation Systems.....	19
3. METHODOLOGY AND MODEL DEVELOPMENT.....	27
3.1 Computational Fluid Dynamics in Industrial Ventilation.....	27
3.2 Ventilation Parameters.....	39
3.3 Model Development and Set Up.....	42
4. RESULTS AND DISCUSSION.....	51
4.1 Grid Independence Analysis.....	51
4.2 Ventilation Performance Analysis of Single-inlet Installation Schemes.....	53
4.3 Ventilation Performance Analysis of Two-inlet Installation Schemes.....	60
5. CONCLUSIONS AND FUTURE WORK.....	68
5.1 Conclusions.....	68
5.2 Future Work.....	69

REFERENCES ..... 71



## LIST OF FIGURES

	Page
Figure 1. Negative pressure ventilation .....	4
Figure 2. Local ventilation system.....	4
Figure 3. Procedure for CFD-based ventilation modeling study .....	8
Figure 4. Illustration of mixing ventilation.....	9
Figure 5. Illustration of displacement ventilation.....	10
Figure 6. Typical supply air speed in different ventilation systems .....	17
Figure 7. Typical supply air temperature in different ventilation systems .....	18
Figure 8. Aspect ratio and biasing for grid .....	30
Figure 9. Examples for local age prediction .....	41
Figure 10. Example for configuration of purging flow rate .....	42
Figure 11. Fine computational grid of scheme 1 .....	48
Figure 12. Velocity contour of coarse-meshed scheme one geometry .....	51
Figure 13. Velocity contour of medium-meshed scheme 1 geometry .....	52
Figure 14. Velocity contour of fine-meshed scheme 1 geometry.....	52
Figure 15. Velocity contour of finest meshed scheme 1 geometry .....	53
Figure 16. Velocity contour of scheme 1 (cross section between inlet and outlet) .....	54
Figure 17. Velocity contour of scheme 2 (cross section between inlet and outlet) .....	54
Figure 18. Velocity contour of scheme 3 (cross section between inlet and outlet) .....	55
Figure 19. Velocity contour of scheme 1 (Cross section at the height of 1 meter) .....	56
Figure 20. Velocity contour of scheme 2 (cross section at the height of 1 meter) .....	56

Figure 21. Velocity contour of scheme 3 (cross section at the height of 1 meter) .....	57
Figure 22. Carbon monoxide mass fraction contour of scheme 1 (cross section between inlet and outlet).....	58
Figure 23. Carbon monoxide mass fraction contour of scheme 2 (cross section between inlet and outlet).....	59
Figure 24. Carbon monoxide mass fraction contour of scheme 3 (cross section between inlet and outlet).....	59
Figure 25. Velocity contour of scheme 4 (cross section between inlet and outlet) .....	60
Figure 26. Velocity contour of scheme 5 (cross section between inlet and outlet) .....	61
Figure 27. Velocity contour of scheme 6 (cross section between inlet and outlet) .....	61
Figure 28. Velocity contour of scheme 7 (cross section between inlet and outlet) .....	62
Figure 29. Velocity contour of scheme 4 (cross section at height of 1 meter) .....	63
Figure 30. Velocity contour of scheme 5 (cross section at height of 1 meter) .....	63
Figure 31. Velocity contour of scheme 6 (cross section at height of 1 meter) .....	64
Figure 32. Velocity contour of scheme 6 (cross section at height of 1 meter) .....	64
Figure 33. Carbon monoxide mass fraction contour of scheme 4 (cross section between inlet and outlet).....	66
Figure 34. Carbon monoxide mass fraction contour of scheme 5 (cross section between inlet and outlet).....	66
Figure 35. Carbon monoxide mass fraction contour of scheme 4 (cross section between inlet and outlet).....	67
Figure 36. Carbon monoxide mass fraction contour of scheme 7 (cross section between inlet and outlet).....	67

## LIST OF TABLES

	Page
Table 1. Industrial hygiene control techniques in chemical plant .....	2
Table 2. Advantages of CFD tools in industrial ventilation study.....	27
Table 3. Boundary conditions usually used in ventilation simulation .....	35
Table 4. Examples for local age prediction .....	42
Table 5. Example for configuration of purging flow rate.....	43
Table 6. Computational geometry of installation schemes.....	44
Table 7. Cell data of different schemes based on different level of mesh quality .....	48
Table 8. Constants setting of two equations realizable k- $\epsilon$ viscous model.....	50

# 1. INTRODUCTION

## 1.1 Background and Motivation

Chemical company and society always want to eliminate the damage to the environment and lower the casualty when an incident occurs. Since there are many public and ethical concerns which are demonstrated in laws and regulations, finding a more efficient and effective way to achieve this goal is now more critical than ever.

### **Industrial Hygiene in Chemical Industry**

Industrial hygiene is a discipline that focuses on the identification, evaluation, and control of the working environment, which can lead to an incident that can cause casualties. It also concentrates on choosing the appropriate equipment and utilize them to monitor the workplace conditions, and control the working environment. There are four elements in industrial hygiene which are anticipation, identification, evaluation, and control.

In any chemical plant or refinery, the industrial hygiene and process safety professionals collaborate closely since industrial hygiene is an essential part of a plants' process safety program. It has been proved that the hazardous materials can be utilized safely if we can apply the technique of industrial hygiene appropriately to every day's production process [1].

### **Control Techniques in the Chemical Industry**

When the hazard identification process is finished, the industrial hygienist should make a feasible plan for the installation of health hazard control techniques. When making

this plan, the appropriate method and instruments should be used to eliminate or reduce the worker's exposure to hazards of chemical plants and refineries.

There are many kinds of industrial hygiene methods in chemical industry. Commonly used techniques are illustrated in Table 1.

**Table 1. Industrial hygiene control techniques in chemical plant [1]**

<b>Methods</b>	<b>Typical techniques</b>
Inherently safer design	Eliminates use of chemical completely. Lower the inventories of the hazardous chemicals. Replace the hazardous chemicals to less hazardous one.
Enclosures	Enclose hazardous processes in to a confined area. Utilize instruments to monitor the inside equipment. Shield and protect the hot surfaces
Local ventilation	Use appropriately designed local ventilation system for charging and discharging. Use local ventilation in drumming station and sample points
Dilution ventilation	Use dilution ventilation to isolate the workplace from the office area. Locker rooms should have proper ventilation and proper enclosure of contaminant.
Wet methods	Clean the workplaces frequently. Use water sprays to protect the pump seals
Personal protection	Use appropriate personal protective equipment (PPE) like safety goggles and face shields. Use the appropriate respirators.

Choosing and designing the appropriate industrial hygiene technique is essential for the safety of the plant and worker. When developing the industrial hygiene technique, the professionals should make sure that the applied methods can successfully work and cannot generate new hazard in the meantime. Sometimes there is a possibility that the new hazard the created by the control method can be even more dangerous than the original problem [1].

## 1.2 Industrial Ventilation System

Ventilation is the most used engineering method for controlling airborne toxic material environmentally. The design of industrial ventilation system is based on two principles; the first is to dilute the airborne explosive and toxic materials lower than specific limitation. The second principle is to eliminate the contaminant before it hazards the health of workers.

There are two main components in ventilation systems which are fans and ducts. The fans can generate a pressure drop which is typically less than 0.1 psi than can move the air. There is definite pressure ventilation system and negative ventilation system. The negative pressure ventilation system is better because it can make sure that even if there is a leak in the system, it still can pull the air out instead of expelling the explosive and toxic materials in, since the fan is located at the end of this system. A typical negative pressure ventilation system is shown in Figure 1.

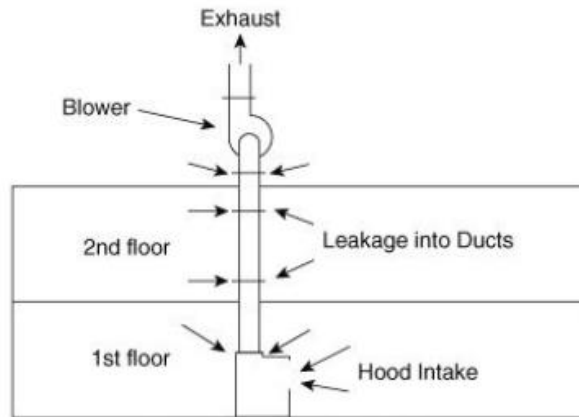


**Figure 1. Negative pressure ventilation [1]**

### Local Ventilation

Local ventilation can cover the source of contaminant entirely and moves the contaminant to an exhaust device [2]. A typical local ventilation system is illustrated in Figure 2.

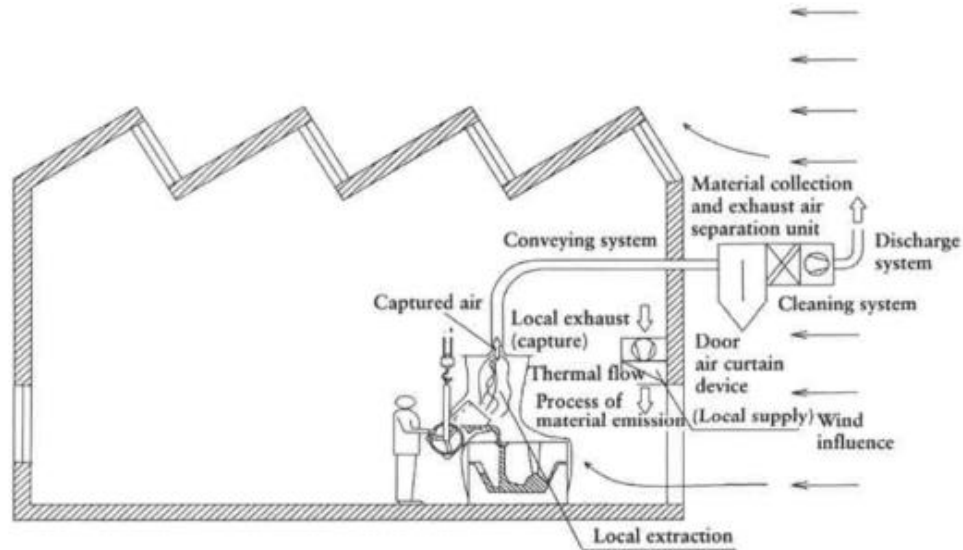


**Figure 2. Local ventilation system [1]**

The design equations for a different type of hood and duct are widely different. Hood is one of the examples. For most situation, assume plug flow when doing the calculation.

The calculation equation is shown below:

$$Q_v = A\bar{u} \quad (1)$$

Where A is the cross-sectional area of the hood and u is the average velocity,  $Q_v$  is the volume flow rate.

When designing a hood, the strategy is to have a constant air velocity at the opening of the hood. It is called “face velocity” or “control velocity” which will make sure that the hazardous vapor cannot escape from the hood.

### **Dilution Ventilation**

If the hazardous material cannot be covered under the hood or it must be used in open space. Dilution ventilation must be used in this kind of situation. The dilution ventilation is not like hood ventilation. Dilution ventilation will make workers exposed to the contaminant, but it will be diluted by clean air. Since the dilution ventilation requires much more air than hood ventilation, the operation cost of dilution ventilation can be substantial.

The calculation equations for ventilation rate are shown below:

$$C_{ppm} = \frac{Q_m R_g T}{k Q_v P M} \times 10^6 \quad (2)$$

$$Q_m = \frac{M K A P^{sat}}{R_g T_L} \quad (3)$$

$$C_{ppm} = \frac{K A P^{sat}}{k Q_v P} \times 10^6 \quad (4)$$

When calculating ventilation rate for multiple sources, we need to compute the dilution air needed separately. The total ventilation rate is the sum of the individual dilution requirements [1].



Dilution ventilation systems are not as effective in controlling contaminant as local ventilation. However, sometimes the dilution ventilation systems are more controllable, which make it more economical than local ventilation system.

### 1.3 Computational Fluid Dynamics

Computational Fluid Dynamics (CFD) is one of the crucial technologies in the field of fluid mechanics. Numerical approaches are used to solve the governing equations of fluid mechanics using computers, and the flow field can be predicted. Currently, there is a variety of CFD software available, such as FLUENT, CFX, FLACS and so on.

Currently, in the field of engineering, CFD methods have been widely used. The most basic consideration of CFD is how to treat the continuous fluid on the computer in a discrete manner. One approach is to discretize the spatial region into cells to form a three-dimensional grid and then apply the appropriate algorithm to solve the equations of motion (Euler's equations for non-viscous fluids, Navier-Stokes equations for viscous fluids, Stokes equation). Also, such a grid may be irregular (e.g., composed of triangles in two dimensions, tetrahedrons in three dimensions) or regular; the former is characterized by the fact that each cell must be stored separately in memory. Finally, if the problem is highly dynamic and spans a broad range of scales, the grid itself should be dynamically adjustable over time, such as in adaptive mesh refinement methods.

### 1.4 Research Objectives

In this research, a confined laboratory geometry is developed, and a dilution ventilation system is installed. The method of Computational Fluid Dynamics has been

used in this research to analyze the fluid dynamic performance in the laboratory using dilution ventilation system.

A variety of different ventilation system installation schemes are proposed, and the performance of different schemes are examined and compared through simulation to get the optimal installation plan for the best contaminant control.

The proposed scheme also optimizes the ventilating system installation by investigating the system's performance with different transmitted mediums. The dilution ventilation system installation scheme is also optimized to fit different contaminant situation. The computational fluid dynamics simulation is a better tool for optimizing the ventilation system. From computational fluid dynamics simulation, we can better understand the flow behaviors of the fresh air intake and contaminant distribution in confined and unconfined space. Therefore, an optimized scheme of industrial ventilation system installation to increase its efficiency in different operation condition is critical.

The results of this research work can serve as references to maximize the ventilation efficiency and minimize the energy cost.

## 1.5 Outline of Research

Figure 3 shows the procedure for CFD-based ventilation modeling study. In the first chapter, background information and motivation of this research is introduced, and this chapter also presents discussion industrial ventilation system and computational fluid dynamics. A general literature review is presented in Chapter 2. This chapter first introduces the development history of ventilation systems and the introduction of different ventilation systems and then gives a brief introduction of the evaluation methods of

ventilation efficiency. Secondly, this chapter also introduces the history of CFD development and application and its application in ventilation system research and design.

The development of dilution ventilation system model in this thesis is described in Chapter 3. The methodology of CFD in ventilation simulation is introduced, and the equation and the simulation setting preference is also discussed in this chapter.

In the last part of Chapter 3, the geometry of the confined laboratory space is introduced, the parameter setting and different scheme of ventilation system installation are proposed.

The results of ventilation simulation and comparison of different installation scheme are discussed in Chapter 4. This chapter also discusses the contaminant's influence on ventilation system performance. Conclusions and suggestions for future work are presented in Chapter 5 and 6.

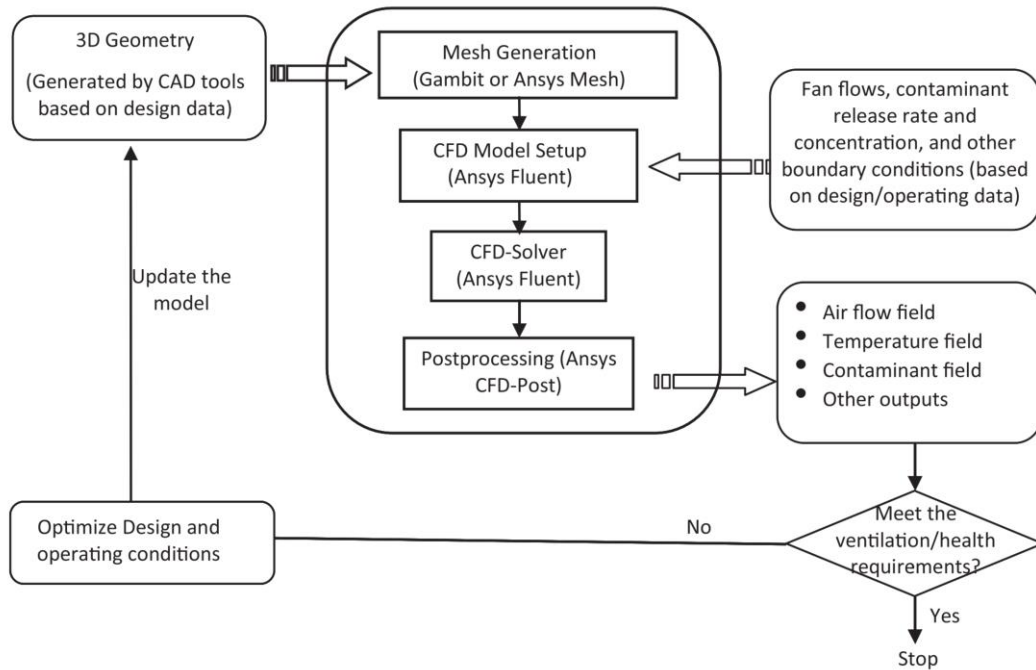


**Figure 3. Procedure for CFD-based ventilation modeling study**

## 2. LITERATURE REVIEW

### 2.1 Industrial Ventilation Systems

#### 2.1.1 Mixing Ventilation

Figure 4 shows the illustration of mixing ventilation system. Mixing ventilation was invented in the 19<sup>th</sup> century and illustrated in 1899 by Boyle Son [3]. In recent years, many formal international standards were developed which defined the mixing ventilation systems in term of thermal comfort and also air quality [4-6]. The fundamental principle of the mixing ventilation is to introduce fresh air to confined space, which can dilute the contaminated air and finally lower the toxic concentration. Practically, inlet airflow and heat source in the room can all influences the dilution. The airflow behavior of mixing ventilation has been already well studied since it was invented in the 19<sup>th</sup> century. The design rules of mixing ventilation system have already been well studied which can make the airborne contaminant quiet concentration consistent within the designated space [7].

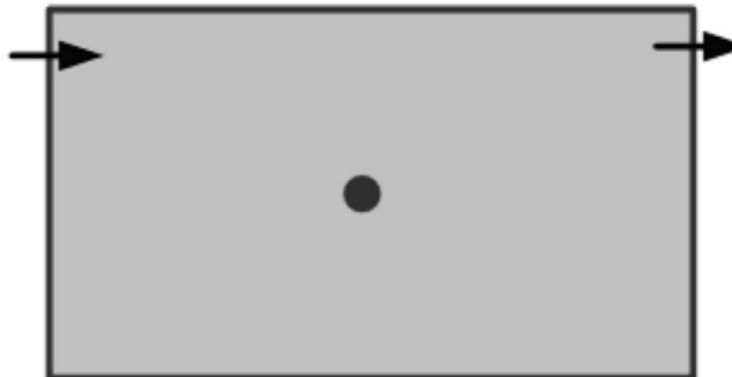


**Figure 4. Illustration of mixing ventilation**

In the 20<sup>th</sup> century, many types of research were conducted regarding the improvement of mixing ventilation [8, 9]. One design guideline was published by REHVA,

which gives us a comprehensive strategy of apply mixing ventilation in ventilation design [10]. Besides, the air diffusion and ventilation performance of air inlet and outlet test standards and procedures are all developed. However, there is no study about the thermal plume's influence on mixing ventilation performance since this effect is always underestimated. There are many cases that when the thermal plume becomes the primary driver, the convective flow will be the main flow pattern of the airflow behavior.

### 2.1.2 Displacement Ventilation

Figure 5 shows the illustration of displacement ventilations. The fundamental principle of displacement ventilation is to remove contaminated air and replace it with fresh air which is different from the mixing ventilation. Temperature oriented calculation method is always used when trying to calculate the airflow of displacement ventilation. The low temperature outside air is supplied at a speed of fewer than 0.5 meters per second, which is a very low the inlet air will tend to move to the top of the room which is called thermal plumes. Due to its airflow property, it will usually form a vertical velocity, concentration and temperature gradient [11-15]. The gradient profiles are dependant on the device user and the distribution of heat source.

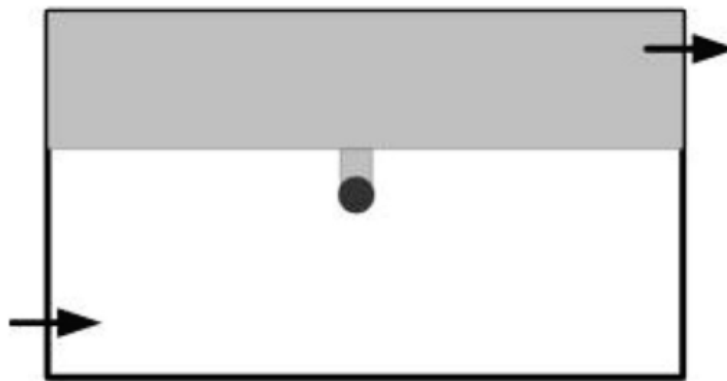


**Figure 5. Illustration of displacement ventilation**

### 2.1.3 Hybrid Air Distribution

Although the displacement ventilation system is a more efficient way to lower the contaminant concentration, it still has two shortcomings that can affect its performance; the first problem is that it cannot be used in a heating mode so it can avoid the full mixing effect. The second problem is that the inlet air cannot be well mixed with air in the room if there is a dominant heat source. Hybrid air distribution system is invented to solve these problems, which combine the advantage of mixing ventilation and displacement ventilation. Some hybrid air distribution system have been invented like impinging jet system and confluent jet system [16-18].

The method of confluent jets has been applied in various industries but only introduced in ventilation industry recently [19]. The confluent jets' definition meteorology is the streamlines pattern that has same wind directions and different wind speed. In ventilation industry, the confluent jets mean when different airflow in the same direction and they will merge into a single jet. The flow behavior of confluent jets in isothermal condition was investigated by experiment as well as numerical simulation [20].

For displacement ventilation system, the airflow will distort when the airflow at the far side from the inlet since the velocity has decreased and there is also temperature stratification effect. So the confluent jets ventilation system will have a more airflow spread than the displacement ventilation and will boost the performance of ventilation effectiveness [19, 20].

## 2.2 Assessment of Ventilation Systems

The evaluation of ventilation system first came up in the 1950s, which measure the effectiveness of removing the contaminants. The effectiveness of ventilation systems depends on many aspects, the indoor layout, the objective of ventilation, the complexity of airflow can all have an impact and the ventilation systems performance [21]. There are four essential elements when evaluating a ventilation system, comfort, contaminant concentration, energy efficiency and air quality, which can also be defined as remove the airborne contaminant, protect occupant and air exchange.

In the early 1980s, a new evaluation method was developed called the age of air, which can quantify the air exchange efficiency for indoor ventilation system [22]. The basic idea of the age of air is to quantify the age problem of airborne toxic and air. Subsequently, many concepts of ventilation system evaluation method were developed since the development of tracer gas method. The ventilation performance has a negative functionality with the tracer gas age, and also the ratio between concentrations [22-24]. A three level evaluation of ventilation performance can be introduced based on the airborne toxic concentration profile so the efficiency of each point in the room can be assessed [24].

In the 1930s, a paradigm was developed as a guideline to improve the comfort of the ventilated room in temperature and contaminant control. The local ventilation effectiveness expresses the ability of a ventilation system at different parts of a room [23].

### 2.2.1 Effectiveness of Contamination Removal

Mean, and absolute ventilation effectiveness is the measurement of ventilation performance in a certain monitor point or area. Contaminant removal ventilation effectiveness is defined as follows: [22, 23, 25]

$$\varepsilon_e = \frac{C_e - C_S}{C_P - C_S} \quad (5)$$

In this equation,  $C_e$  is the toxic concentration of outlet airflow,  $C_S$  is the toxic concentration of inlet air and  $C_P$  is the toxic concentration of designated area. For example, the ventilation effectiveness equation can be used to calculate the toxic vapor removal efficiency if  $C_P$  is the breathing level concentration. Since both  $C_P$  and  $C_S$  are in denominators, the efficiency value will tender to be infinity large when  $C_P$  and  $C_S$  are equal. If we want to have the transient ventilation efficiency at a certain point of time, the absolute ventilation efficiency is introduced, the equation is shown below: [25]

$$\varepsilon_a = \frac{C_{pi} - C_{pt}}{C_{pi} - C_i} \quad (6)$$

$C_{pi}$  is the initial concentration at the point you want to calculate,  $C_{pt}$  is the concentration after time t,  $C_i$  is the inlet air concentration. There is also one study which uses the contaminant concentration increase rate at a certain time as the ventilation effectiveness when the release rate of contaminant and ventilation rate is known and perfect mixing assumption is applied [27].

Another research came up with a dimensional indicator to demonstrate the ventilation effectiveness for removing toxic materials performance.

Local purging flow is used when doing ventilation simulation, and the concept of net escape velocity was introduced recently, which is an extension of evaluating ventilation effectiveness [26, 28].

Net escape velocity is a coefficient derived from purge flow rate of the ventilation system, which is used for evaluating the performance of contaminant removal for ventilation system [26, 28].



The net escape velocity also can be used in describing ventilation effectiveness which is more usually used in expressing the effectiveness of contaminant removed. When calculating this indicator, the flow rate of inlet air and the flow rate at the designated point is needed. The equation of local purging flow rate is shown below:

$$U_p = \frac{Q_{ce}}{C_p} \quad (7)$$

$U_p$  has the same unit as the inlet air flow rate which is  $m^3/s$  or  $kg/s$ ,  $Q_{ce}$  is the outlet air concentration,  $U_p$  has the same units as  $Q$  (air supply rate), namely  $m^3/s$  or  $kg/s$ ,  $C_e$  is the pollutant concentration in exhaust air,  $C_p$  is the average contaminant concentration in the designated area.

Since the source or contaminant will vary from a different case, there are three different levels of ventilation efficiency are introduced which is SVE1, SVE2, and SVE3 [78]. SVE 1 is the level that means that the diffusion of the contaminant was started from a point source. SVE2 means the average diffusion radius of the contaminant and SVE3 is the average time that the contaminant reaches the point of concern, especially when the contaminant diffusion is uniform across the whole region [29].

### 2.2.2 Air Exchange Effectiveness

Air exchange effectiveness is used to evaluate the time that the fresh inlet air reaches the designated point at the room which means the average time that the inlet air will displace the contaminated air. The equation of calculating the air exchange effectiveness is shown below [30]:

$$\varepsilon_a = \frac{\tau_n}{2\tau_p} \quad (8)$$

In this equation,  $\tau_n$  is the nominal time constant for the room, the time constant is the reciprocal of the air change rate, which is equal to Q divided by V, which is shown in the equation below.  $\tau_n$  can be calculated by the inlet air supply rate Q divided by the volume of the confined space V [22], and  $\bar{\tau}_p$  mean the average residence time of the air.

$$\tau_n = \frac{V}{Q} \quad (9)$$

The average residence time of the air can be calculated from the equation below:

$$\tau_p = \frac{1}{C(0)} \int_0^{\infty} C_p(t) dt \quad (10)$$

In this equation,  $C(0)$  is the tracer gas concentration at the beginning, and  $C_p(t)$  is the contaminant concentration at the designated position after time t.

### 2.2.3 Scales of Ventilation Systems

The ventilation systems selection need to be based on the situation, the different situation has different thermal condition, different pollutant, and the geometry of the room is also different.

The personalized ventilation concept was also developed by some researches which is also called the personal exposure effectiveness ventilation [31, 32]. It is because the fresh inlet air needs to be supplied directly to the occupied area.

In that case, the scale of the ventilation needs to be small enough instead of a large one like another ventilation system. However, the dilution ventilation can introduce the fresh air into the room, which can lower the contaminant concentration to an acceptable level which can be applied to the whole occupied area. The fundamental principle of the displacement ventilation is to remove the contaminated air and replace it with fresh air [33],

which makes the displacement ventilation system accessible to a specific area. The local exhaust ventilation can be used as add-on equipment that can be very useful for the situation that the diffusion source is recognized and localized like lab hood. However, the contaminant source in confined space is usually unknown.

The thermal plume created by human body breathing which can affect the airflow property significantly can also change the concentration profile of the toxic. The protection ventilation is used to keep the occupant away from the contaminated air.

#### 2.2.4 Effectiveness and Efficiency of Different Ventilation Methods

To evaluate the performance of ventilation system, five indexes were developed which includes the air exchange ventilation effectiveness [34], contaminant removal ventilation effectiveness [22, 27], heat removal ventilation effectiveness [23], exposure ventilation effectiveness [31] and the index of air distribution. In recent years, there is another index that has been introducing to test the effectiveness of ventilation system [35]. For the application of ventilation system, the choice of the ventilation system is fundamental since it can significantly affect the performance. One example is the effectiveness of toxic removal. There is research that shows that the toxic removal effectiveness can be reduced due to the flush-out effect which means that the effect will recirculate the toxic in the room so it cannot be removed [36]. In practice, almost every ventilation system can be evaluated by more than two indexes. Since the primary purpose of the protective ventilation system is the protect the workers from toxic in the confined workplace, the primary way to enhance this kind of ventilation system is to reduce the exposure of contaminant and improve the air quality of the particular area.

### 2.2.5 Application of Ventilation methods with Different Contaminant Sources

Figure 6 shows the typical supply air speed in different ventilation systems. The primary purpose of the ventilation system is to lower the contaminant concentration to an acceptable level, sometimes, the heat created in the room also can be considered as a contaminant. There is no doubt that the situation of indoor contaminant can affect the performance of ventilation system significantly. Various kind of chemical substance can be harmful to human health which includes the production of chemical, building material, smoke and dust from process unit [29]. Figure 7 shows typical supply air temperature in different ventilation systems.

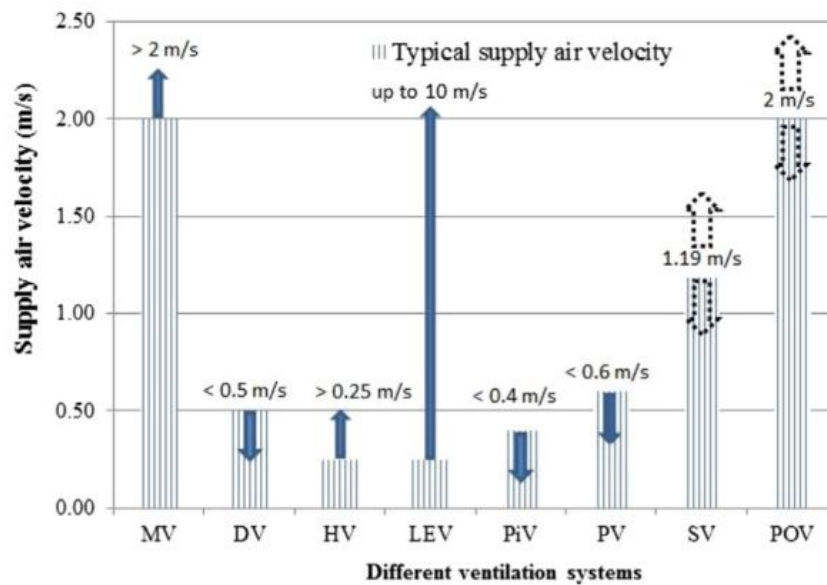


**Figure 6. Typical supply air speed in different ventilation systems [29]**

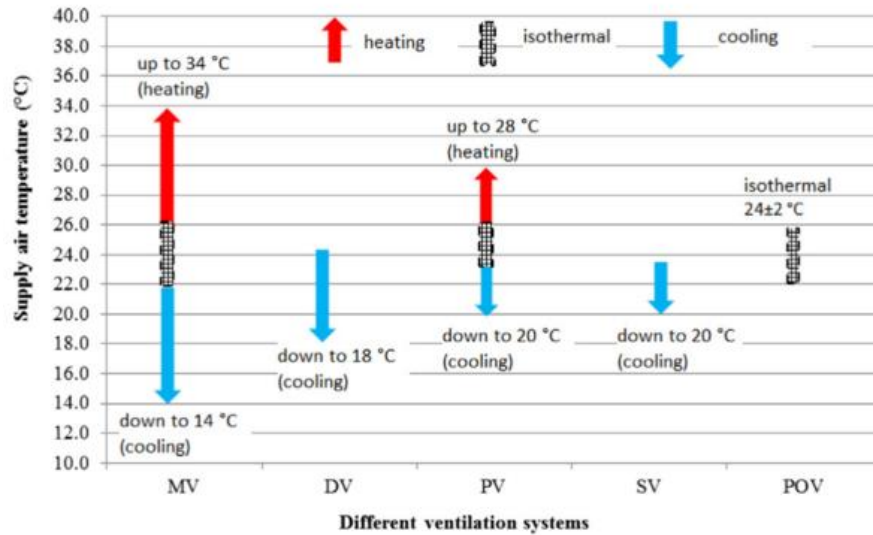


**Figure 7. Typical supply air temperature in different ventilation systems [29]**

Many chemicals can cause an allergic reaction of people and there are also some of them like volatile organic compounds (VOC), which can highly irritate the mucous membranes [37]. Apart from that, the contaminant source can also be affected by the thermal power in the room, which can form an active source of contamination [38]. Displacement ventilation can be more effective in the room involved in active contaminant source than passive contaminant source [38]. However, the risk may increase if the room only has the slow vertical speed ventilation [39].

Fig. 6 indicates the typical speed of inlet air, apart from mixing ventilation and LEV the inlet airspeed usually is lower than 2.0 m/s. For mixing ventilation, the inlet of the ventilation system can be on the outside of the confined space. For other different kinds of ventilation system where the air inlet is located inside the room, the supply airspeed needs to be limited [40].

### 2.3 Simulation and Computational Techniques for Ventilation Systems

Ventilation plays a vital part in safety and chemical engineering. It is essential to profoundly understand the contaminant vapor and air flow behaviors when designing the chemical plant. The flow behaviors can be obtained from conducting tests in wind tunnels or by having experimental simulations. However, conducting these experiments can be very uneconomical. Besides, the results of these simulations may be different from the actual situation, since experimental scaling procedure is not very accurate [41].

Using numerical simulation is another way to investigate the flow behaviors and ventilation rate in the plant [42]. Numerical simulations can be realized through computational fluid dynamics (CFD), which is a very efficient, economical and precise method. Computational fluid dynamics is broadly used in plant design, process control. In complicated air flow situation, it has been proved that the simulation results are accurate and acceptable [43].

Nowadays, computational fluid dynamics is often used in hazard identification and critical condition area classification. Ronald's study of simulations for outdoor and open environments is a useful application of computational fluid dynamics. The author used a 50,000 nodes simple model to simulate an offshore oil platform in aspects of gas dispersion, air flow, and ventilation [44]. Besides, Eslam Kashi analyzed gas dispersion behaviors and possible hazards after dispersion; then he used computational fluid dynamics method to identify hazards in different ventilation conditions [45]. Khan studied the different locations' influence on ventilation air intake and outlets on the dispersion of light or heavy gas by the computational fluid dynamics model. The U.S. Environmental Protection

Agency (EPA) also conducted successful studies and simulations on natural ventilation in an urban environment [46].

Many papers about behaviors of air and dust contaminant have been published. However, the application of computational fluid dynamics immensely improved and accelerated these studies. The behavior of contaminant particles is readily determined and visualized in urban environments [47].

Paul Gilfrin and Erin Hatfield use computational fluid dynamics method to simulate the ventilation situation in massive Sheffield City Hall. They believe that this method can visualize the simulation and make the results more understandable. They also used the visualization results to present their research in 2005 [48].

We also need actual experimental data to verify our results from computational fluid dynamics simulation. Many researchers studied in their field and discovered the applications of computational fluid dynamics [43, 44, 49-52].

Numerical simulation methods and computational modeling are being widely utilized in industrial ventilation design, optimization, construction, and research for many years. These methods are developed to enhance and assist the ventilation system design with relatively low cost [1]. Before the time when computational fluid dynamics was developed, researchers and engineers could only rely on hand calculation and extrapolations in extending a design beyond conventional concepts [2]. In late 20<sup>th</sup> century, with the rapid development of computer technology and graphical user interface (GUI), which made the computer modeling affordable and possible in both research and industry [3], this development has dramatically facilitated the overall progress of ventilation simulation.

### 2.3.1 Analytical method

The analytical method has been widely applied to natural ventilation design and research. Li. use analytical method to solve the flow properties of combined wind and buoyancy forces driven natural ventilation in a two-opening single-zone building [53], they also use the same method to solve the analytical solution for three different two opening building structure and compare the solution with the experimental results [54]. Chen . use the analytical method to solve the solution for the single-zone building which has three different level openings with displacement ventilation, they also provided an optimization guide for the same structured buildings [55]. For uniform temperature, thermal buoyancy driven natural ventilated room with two openings are also solved for analytical method [56]. Furthermore, a solution for opposing wind-driven natural ventilated room with openings are also derived [57]. Leung developed a simulation model for both natural and hybrid ventilated simple structured building. The analytical method can also be used in other situation like solar chimney [58] and thermal stratified natural ventilated room [59]. Those analytical model all need a temperature input for the solution.

Analytical methods can also be applied in solving the contaminant concentration profile in a ventilated room. Mazumdar derived a one-dimension model for airplanes cabin contaminant concentration and transportation properties using analytical methods [60] which includes not only the diffusive transport effect but also the convective transport of contaminants. Parker used the analytical models to solve the concentration profile for airborne substance in multi-zone buildings [61]. The simulation results indicate that highest zone exterior air change rate can predict the maximum concentration. Nazaroff also used analytical methods in his work to estimate the fraction of airborne toxic for indoor



environment situation [62] to solve the risk of exposure for the people in the polluted building[63].

However, the application of the analytical model to solve ventilation problem is also constrained by incomplete understanding of physics. So researchers added some new parameters or empirical rule to the analytical model to improve the former models.

Bastide [64] used the CFD to simulate the flow properties in a cross-ventilated room with two large openings and compared the result with the mass and heat transfer solution obtained from the Walton model. He introduced a parameter for the kinetic energy into the simulation, so the prediction quality and the simulation results showed that this additional parameter increases the accuracy better agreed with the mass flow and air pressure.

### 2.3.2 CFD approach

Computational fluid dynamics (CFD) was first used in ventilation system simulation in the early 1970s. However, it was substantially facilitated in the 1990s since it is the time that many CFD software were developed and the calculation speed of computer has increased a lot, which makes more complex CFD simulations possible. Besides, the hardware cost also reduced significantly which makes the CFD simulations more accessible. CFD is also very useful in ventilation system modeling since it can give the designer and researcher a visual and quantitative result of flow properties which can be highly useful for ventilation system optimization and design assistance. CFD methods are primarily used in simulating and predicting airflow pressure, velocity, and its temperature. It also can calculate the concentration profile of the contaminant in indoor and outdoor situations. There are many types of research and reviews conducted concerning the CFD

application in the ventilation system. This means that the CFD application in ventilation simulation has now raised more and more interest for ventilation system design and research. Nowadays, the application of CFD is a must for intricate ventilation system design and optimization of ventilation system [65]. Norton has reviewed CFD applications for research and industries in 2006 and 2007 [66, 67]. Nielsen also reviewed the application of CFD in investigating the air flow distribution for past 50 years [68].

The fundamental principle of CFD is to solve the fluid flow governing equations. However, the accuracy of the simulation result and the calculation speed for solutions can be affected by many factors like meshing quality, model set up and scheme of discretization, turbulence model.

#### 2.3.2.1 Turbulence Modeling

Turbulence modeling is essential for ventilation system CFD simulation which can affect the accuracy of solution. Using the appropriate method of turbulence modeling in ventilation system simulation can significantly improve the calculation speed and can increase the accuracy of the simulation result as needed.

The most used turbulence model for CFD simulations research is the Reynolds Averaged Navier Stokes (RANS) turbulence model. It is also accompanied with different kinds of the  $k - \epsilon$  model which identified by researchers. Brau [69] in his research used four different two-equation model to the test the accuracy of the simulation and Murakami [70] validates the simulation using  $k - \epsilon$  model by comparing the simulation results with experimental data

Improving turbulence model to increase the accuracy of ventilation system simulation is always an important objective for researchers. Moreover, there is much progress for doing that, in 1998, Chen [71] developed an empirical model that does not include any equation that can apply to the confined space simulation using mixed length hypothesis. This method assumes that the eddy viscosity is a function of the length scale and the velocity of the fluid flow. This turbulence model can reduce a tremendous amount of calculation load and the cost of the simulation. Moreover, it is also proved to fit the experimental data accurately. The equation 5 is the expression of Chen's turbulence model.

$$v_t = 0.03874uL \quad (11)$$

Since the hardware for the computer is growing, which can make them a more complex turbulence model applied in CFD simulation possible. Large eddy simulation (LES) is one of the models that were greatly facilitated due to the development of the calculation capability of the computer. LES model uses the spatial filtering operation to categorize different sizes of turbulent flow which is different from RANS model. In recent years, detached eddy simulation (DES) method is developed and confirmed in especially natural ventilation that it is a better way to improve the accuracy of the simulation. The DES model took advantage of both RANS and LES models [72]. Moreover, it is also more effective and accurate in the simulation of displacement ventilation system [73].

There is no turbulence model that can be universally applied since the different structure of room have a different condition of flow behavior, and different models have their condition-specific parameters, and empirical assumptions applied. In that case, we need to have a more comprehensive understanding of the application situation of different turbulence models. Many articles have compared and discussed the application of different

turbulence models in different conditions. Chen compared different simulation results using various  $k - \epsilon$  models for confined space ventilation airflow by test the results' fitness for experimental data, simulations turn out that the RNG  $k - \epsilon$  model have the best fit to the experimental data [74]. There also a study comparing the CFD simulation results of 20 different most-used RANS, LES and, DES turbulence models for estimating the behavior of indoor ventilation flow [75] and also validate the results against experimental data [76]. The conclusion provides good guidance for subsequent CFD users in selecting the proper turbulence model for indoor environment modeling.

#### 2.3.2.2 Computation Grid

The grid of the simulation geometry is also critical for an accurate CFD simulation result. To eliminate the effect of the mesh size on simulation results, a grid independence test needs to be conducted [77].

A refinement or a more detailed grid is needed for flow near the boundary conditions and where the flow gradient is high [78]. At the area where a large gradient of flow velocity, pressure or temperature can be expected, meshing should also adapt to fit the high gradient change so the simulation results can be more accurate [79]. However, an over-detailed grid can highly increase the time and cost calculation. Choosing a right grid resolution is also a part that needs more research [80].

#### 2.3.2.3 Air Contaminant Modeling

CFD not only can be very useful for predicting the airflow behavior but also can be applied in simulating the concentration profile of airborne contaminants. Toxic materials that can be transmitted through the air can profoundly affect worker's health and life. In

recent years, there are many studies regarding the control of toxic release by using CFD simulation. Since the airborne toxic gas like VOC has a continuous distribution among the indoor environment [81], so the Eulerian regime can be applied when simulating at this condition. When doing simulation for the confined places toxic material concentration profile, the Eulerian and Lagrangian methods can be applied to this situation [82, 83] with the use of RANS turbulence model if the toxic gas distribution is discontinuous. To increase the prediction accuracy of the toxic gas distribution, both LES model and Lagrangian method are combined to test its effect on simulation for species transport [84]. The drag force of gas particles is dependant on their particle size. The ventilation effect is different between different size particles [85].

### 3. METHODOLOGY AND MODEL DEVELOPMENT

#### 3.1 Computational Fluid Dynamics in Industrial Ventilation

Computational fluid dynamics (CFD) is a useful tool to assist analysis and design of industrial ventilation system. CFD tools can be utilized in problems when the spatial distribution of flow quantities is need. In other words, it can be used in the situation where local values at different places are needed. The property of the airflow typically includes the velocity, temperature and the concentration of airborne explosive and toxic material such as carbon monoxide, smoke or other toxic and explosive gases. The two essential features of CFD include: data of local quantities and a limited number of physics assumption. Advantages of CFD simulation is shown in Table 2.

**Table 2. Advantages of CFD tools in industrial ventilation study**

<b>Advantage</b>
1. Detailed analysis is possible with CFD.
2. CFD tools can be applied to widely different and complicated situations.
3. The interaction of different flow can be automatically considered as jets, plumes, and boundary layers.
4. CFD tools can find out the problem in advance, even before it can be detected.
5. CFD parameter can be easily varied to suit the different situations.

Easily-controlled parameters is a standard advantage for all numerical analysis methods. Thus, it is much more convenient over experimental methods since it only takes a little effort to change the parameters [86].

### 3.1.1 Grid and Equation

#### 3.1.1.1 Grid

The first step in the application of CFD to solve ventilation problems is to grid the domain. Different flow type will need a different number of grid nodes, and the number needed also depends on the accuracy that the researchers want. The grid is discretized by governing equation, the reliability of the result has a positive relationship with the grid quality. A  $30 \times 30 \times 30$  grid is enough if researchers only need a rough result of the flow field simulation. However, the grid should be optimized especially when there is a significant gradient in the field which means that the grid is usually refined at the area near the boundary or the inlet area.

The discretization scheme is also significant to get a reliable result. In most commonly used CFD software, the discretization scheme can be easily modified. There are two types of schemes that are used very often; one is the first order upwind/hybrid scheme or second order upwind/QUICK scheme. The second order scheme is much more accurate than the first order one, but the stability of the first order scheme is higher than the second order scheme. An appropriate strategy of using the discretization scheme is to use the first order scheme first to see if this scheme can converge the simulation result.

When using a coarse grid, the wall function can be used as imposing boundary conditions. The nondimensionalized distance of wall needs to be  $30 < y^+ < 100$ , where  $y^+ = u_* y / \nu$ . Since the friction velocity is changing with flow, we are not able to calculate the friction velocity  $u_*$  before the simulation. But we can first make an estimation of the  $y^+$  so we can determine the first grid node which is close to the wall at  $30 < y^+ < 100$ .

We can assume that the friction velocity as  $u_* \cong 0.04U_{max}$  if the maximum velocity of the

boundary layer can be obtained or estimated. The result can be validate after the simulation is finished in order to check that the grid node close to the wall satisfy the condition  $30 < y^+ < 100$ .

To have higher reliability and accuracy, the cost of the simulation will increase since there is more computing cost and more grid nodes are needed. The extra node of the grid should be added at the place that the flow behavior is complicated. If the room is empty without any additional obstacle, the extra nodes should be placed near the wall of the room and the inlet area. The extra node is needed if we count the heat transfer of the wall. A Low-Reynolds-Number model should be used when we are considering adding more nodes to the wall. In this particular situation, the grid node position should satisfy the condition of  $y^+ \cong 1$  near the wall. Since we cannot calculate the friction velocity as stated previously but an estimation is always an option. When the simulation is finished, the friction velocity can be calculated since the velocity in the sublayer is liner, which is shown in Equation 1.

$$\frac{U_p}{u_*} = \frac{u_* y}{\nu} \Rightarrow u_* = \sqrt{U_p \nu / y} \quad (12)$$

The high aspect ratio cannot affect the result of simulation but biasing can make the simulation results inaccurate which is shown in Figure 8. The recommended biasing ratio should be lower than 1.1 which means that the size of one cell cannot be more than 10% larger or smaller than the adjacent cell [86].



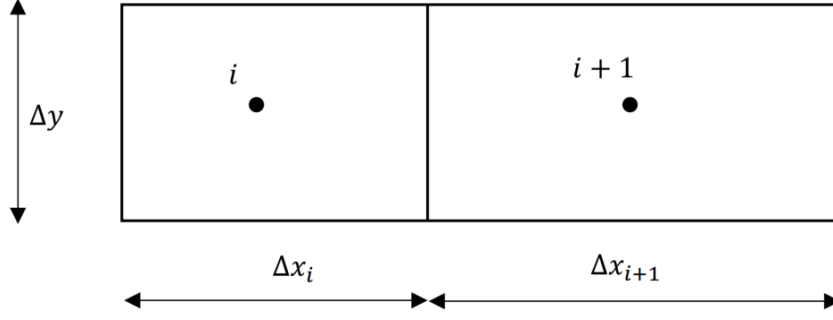


**Figure 8. Aspect ratio and biasing for grid**

### 3.1.1.2 Equations

The Navier-Stokes equations for incompressible, time-averaged continuity is:

$$\frac{\partial \bar{U}_j}{\partial x_i} = 0 \quad (13)$$

$$\frac{\partial \bar{U}_j}{\partial t} + \frac{\partial}{\partial x_j} (\bar{U}_j \bar{U}_i) = -\frac{1}{\rho} \frac{\partial \bar{P}}{\partial x_i} + \frac{\partial}{\partial x_j} \left[ v \left( \frac{\partial \bar{U}_i}{\partial x_i} + \frac{\partial \bar{U}_j}{\partial x_i} \right) - \overline{u_i u_j} \right] + g\beta \delta_{i2} (T - T_{ref}) \quad (14)$$

$$\frac{\partial \bar{T}}{\partial t} + \frac{\partial}{\partial x_i} (\bar{U}_j \bar{T}) = \frac{\partial}{\partial x_i} \left[ \frac{v}{Pr} \frac{\partial \bar{T}}{\partial x_j} - \overline{u_j t} \right] \quad (15)$$

$$U_i = \bar{U}_i + u'_i \quad (16)$$

$$P = \bar{P} + p' \quad (17)$$

$$T = \bar{T} + t' \quad (18)$$

$\beta$  is the inverse of Kelvin temperature scale, because of that:

$$\beta = \frac{1}{273 + T_{ref}} \quad (19)$$

The  $x_2$  coordinate represent the height. On the right side of equation (7) and (8), turbulent stresses  $\overline{u_i u_j}$  and  $\overline{u_j t}$  are stated. These two terms are extra terms that can add diffusion because the relation between the fluctuating velocities and temperature cannot be

obtained. The Navier-Stokes equations can be derived to  $\overline{u_i u_j}$  and  $\overline{u_j t}$ . The higher order relations that cannot be obtained directly are modeled which is called Reynolds stress model.

When using CFD tools to solve the ventilation problem, a more straightforward turbulent model can be used, like eddy-viscosity models. Because of that, the turbulent viscosity term can be introduced, and equation (7) and (8) can be rewritten as follows:

$$\frac{\partial \overline{U}_i}{\partial t} + \frac{\partial}{\partial x_j} (\overline{U}_j \overline{U}_i) = -\frac{1}{\rho} \frac{\partial \overline{P}}{\partial x_i} + \frac{\partial}{\partial x_j} \left[ (v + v_t) \left( \frac{\partial U_i}{\partial x_j} + \frac{\partial U_j}{\partial x_i} \right) \right] + g\beta\delta_{i2}(T - T_{ref}) \quad (20)$$

$$\frac{\partial \overline{T}}{\partial t} + \frac{\partial}{\partial x_i} (\overline{U}_j \overline{T}) = \frac{\partial}{\partial x_j} \left[ \left( \frac{v}{Pr} + \frac{v}{Pr_t} \right) \frac{\partial \overline{T}}{\partial x_j} \right] \quad (21)$$

The mostly used eddy viscosity turbulence model is the  $k - \epsilon$  model and  $k - \omega$  model. In these model, the eddy viscosities term is as follows:

$$\mu_t = c_\mu \rho \frac{k^2}{\epsilon} \quad k - \epsilon \text{ model} \quad (22)$$

$$\mu_t = c_\mu \rho \frac{k}{\omega} \quad k - \omega \text{ model} \quad (23)$$

There is no need to solve the temperature equation in a situation that the isothermal flow is present. In that situation, the last term in equation 13 can also be eliminated. However, if the simulation is done in a thermal comfort condition, then the temperature equation must be solved. In most normal operation of the ventilation system, the temperature change is usually minimal, so it is enough if we only take the density variation into account by using gravitation term, which is the last term in equation 14. The gravity only acts in the vertical direction and the  $x_2$  term in equation 14 has already assumed that it is vertically upwards. The  $T_{ref}$  in the equation is the reference temperature so it should be constant. The  $T_{ref}$  term will not affect the simulation results as long as the pressure does

not change. However, this term may have influence on the convergence rate which is because extra iteration will be needed in order to get a converged solution. Besides, the reference temperature needs to be chosen carefully and it is usually the inlet temperature.

The unit of every term in the temperature equation is joules per unit volume per second,  $J/(m^3 s) = W/m^3$ , because the equation is derived from the energy equation. The temperature equation which is shown in equation 14 has already been divided by the  $c_p$  and  $\rho$ , which is assumed to be constant. Because of that, the unit of each term in equation 14 is  $^{\circ}C/s$ . If a heat source is needed in the simulation, the term of the heat source need to be divided by  $c_p$  which is  $1006 J/kg K$  for air [86].

### 3.1.2 Geometric Modeling and Boundary Conditions

There are some minimum input that is required to run the simulation. If a higher quality result is needed, additional information is required. Usually, the required input is:

1. Geometric modeling
2. Boundary condition

Boundary conditions include the space boundary conditions and spatial boundary conditions like flow, thermal, and mechanical.

The better the quality of the geometric modeling and meshing of the geometry, the better the results of the simulation. There are also models that need to be included in the CFD code and specific boundary conditions that needs be considered.

A reliable and accurate simulation depends on how researchers deal with these problems, the boundary condition is sometimes not easy to find, mainly when the surroundings are naturally ventilated, the boundary condition will be unknown. We can deal with the situation in certain ways. First, the researchers can choose a boundary

condition based on their knowledge and information given. Alternatively, they can use different parameters to conduct the calculation to determine which one is more important. The researchers also have the choice of expanding the system so they can get a better quality result.

The last solution is apparently the best way to do if it is possible, but it also needs to depend on the availability of the model and resources that can be fitted in. One example of such procedures is:

When the room has leakage in the winter season for an unknown amount, multizone airflow models need to be applied to get the simulation calculated. Moreover, another way to solve the temperature of wall or glass that are unknown is to use the specific program for the thermal building. We can also add the solar heat source term which can include the solar distribution [86].

#### 3.1.2.1 Geometric Modeling

Geometric modeling is the first step of ventilation simulation modeling, and it is also an essential step in every CFD simulation since it is the primary step of the computational mesh. An appropriate resolution of the meshing should be chosen based on the availability of current data. The data is always limited so in that case, we have to lower the level and focus on the simulation that can be done with data that is currently available.

Some factors that need to be considered when doing geometric modeling are described belows:

1. The room geometry is essential since we cannot use orthogonal meshes in an inclined wall.

2. Obstacles in the simulating room need to be treated carefully because it might create nodes that cannot be used. Different meshing method will have a different result.
3. Things that are partially blocked like the grill of the air inlet or the vent should also be taken into consideration.

The moving obstacles in the simulation geometry are usually unacceptable. However, the problem can be fixed by employing the adaptive mesh method [86].

### 3.1.2.2 Boundary Conditions

The boundary conditions of the flow are the conditions that govern the flow, so it is crucial in ventilation CFD simulation. Scalar value and flow value for each condition are listed separately in Table 2. The Table also contains the data for volumetric sources which is not a boundary condition technically, but it is often used to define the simulation which has the same function as a boundary condition [86].

#### **Physical Boundary Conditions**

Several types of boundary conditions are used in ventilation CFD simulation. Inflow boundary condition, which is used for the supply of air. The pressure, velocity, and mass of the inlet flow need to be specified for simulation. Moreover, these values also have an associated scalar value that contains the temperature and the concentration of airborne toxic materials. Table 3 shows the boundary conditions usually used in ventilation simulation.

Outlet boundary condition that defines the air flow for the outlet air. The mass flow and velocity need to be specified. The incompressible flow assumption needs to be applied which means that the pressure is constant if there is only one outlet and the pressure of the

outlet flow. If there is more than one air outlet, the pressure difference of the outlet needs to be considered. If the outlet flow parameters are known, the simulation flow is easy to define and represented.

**Table 3. Boundary conditions usually used in ventilation simulation**

<b>Boundary condition type</b>	<b>Flow value</b>	<b>Scalar value</b>	<b>Special issues in ventilation</b>
Inflow	$m, v, \text{ or } p$	$T, C_i, \text{ turb}$	Inlet-box method
Outflow	$m, v, \text{ or } p$	—	
Large opening	$p_{total}$	$T, C_i, \text{ turb}$	Outside flow combined
Wall	$v = 0$	$T, \text{ or } q$	Heat flux or temperature
Volumetric source	—	$q, S_c$	Simplification
Symmetry	—	—	Used when to have subdivision of large hall
Periodicity	—	—	

$m = \text{mass flow}, v = \text{velocity}, p = \text{pressure}, T = \text{temperature}, q = \text{heat flux},$

$C_i = \text{concentration of contaminant species } i, S_c = \text{contaminant source},$

$\text{turb} = \text{turbulent quantities}$

Large opening, there is a special effect that can happen which is called bidirectional flow, the temperature gradient between two rooms causes it. We can take this effect into account if we know the pressure difference between this two-room which includes the static pressure and dynamic pressure. If we have a large opening in the room, we need to expand our calculation to the domain that is larger than the opening to obtain an accurate result.

It is essential that the wall boundary conditions be taken into account since the friction of wall can slow the flow velocity. When encountered temperature boundary conditions of

the buoyant flow which is very often, the wall boundary condition will become more critical.

The moving parts in the simulated area can be considered as a moving wall which can refine the simulation to a more reliable result.

Volume source boundary conditions are the way to process the heat or toxic material source. If we use the volume source boundary condition, we will consider the small source as a part volume of flow which will simplify the simulation.

Symmetry and periodicity boundary conditions are often used to reduce the calculation load of simulation which means that the geometry can be reduced. However, this boundary condition can be used only if the geometry meets the criteria [86].

### **Wall Boundary Conditions**

The most commonly used way to process the wall boundary conditions is to refine the grid mesh so the wall gradient problem can be adequately solved. However, if we want to simulate the complicated 3D flow, refining the grid will enormously increase the calculation load for the computer. Alternatively, additional assumptions can be made to solve the dilemma; we can assume the flow behaves like fully developed turbulent flow. In this case, we can use the prescribed boundary conditions. Since the computational resource is limited, so the nodes number is limited too. The wall functions can be used to refine the grid so there are only a few nodes needed at the wall area so we can apply the spared nodes to the part where the flow gradient is much higher. Moreover, the computer calculation load can be substantially reduced and the simulation time can be reduced too. When we are using wall function to solve the wall area problem, it will assume that the boundary layer near the wall is not resolved and the nearest node to the wall is located at

the boundary area where  $30 \leq y^+ \leq 100$ . Airflow between the node and wall will be considered as flat boundary layer flow. In most cases, it can fit the actual conditions very well but sometime it does not fit the flow behavior at all. When we are using the wall function to process the wall area, the velocity will be computed by log-law, which is shown in equation 17.

$$\frac{U_P}{u_*} = \frac{1}{\kappa} \ln \left( \frac{E u_* y}{\nu} \right) \quad (24)$$

In this equation,  $U_P$  represents the vertical velocity in the node near the wall,  $y$  is the distance from the node to the wall,  $\kappa$  is the von Karman constant which is 0.41, and the  $E$  value is equal to 9.0. The friction velocity  $u_*$  also need to be computed. It can be done by trail and error process. First, a  $y^+$  should be guessed to calculated the  $u_*^{old}$ . Then we can obtain a new friction velocity  $u_*$  by using equation 18.

$$u_* = \frac{\kappa U_P}{\ln(E u_*^{old} y / \nu)} \quad (25)$$

By repeating this process several times, the result will converge and the more accurate friction velocity  $u_*$  can be obtained.

When doing ventilation CFD simulation, the light effect always exists [86].

### **Low Reynolds Number Turbulence Model**

Wall functions are always used to reduce the calculation loads by reducing the nodes needed. However, this is only an approximation to process the wall problem when the flow near the wall is essential to investigate. In many cases, the flow will be within the boundary of walls or symmetry planes, so the boundary layer is not that important at all since the pressure is always dominating the flow field. When doing heat transfer simulation, using wall functions will have an adverse effect on the simulation since the wall function will



predict the convective heat at the wall area. The reason that this error could happen is that that the convective heat is very sensitive to the near-wall area.

At the area near the wall, the viscous effect cannot be ignored, and it is comparable to the turbulent diffusion if the  $y^+ < 5$ . In this case, the assumption of high Reynolds number model is no long accurate since this model assumes the flow is fully developed turbulent flow. A modified model is need to fix that problem, which is call the low Reynolds number model. The Reynolds number in this term is the local turbulent Reynold number which is  $Re_l = Ul/\nu$ ,  $U$  means the turbulent velocity fluctuation and  $l$  means the turbulent length scale [86].

### **Time-Dependent Boundary Conditions and Initial Conditions**

If the parameter is varying with time, the boundary condition can also be time dependent. This kind of conditions like heating cycler can be written as a time-dependent function.

If the simulated ventilation process is a steady-state process, then the initial condition is a minor part of the simulation. However, an appropriate guess of the initial condition can converge the simulation faster.

In ventilation simulation, there are always some regions where the turbulence is very low. In that case, we can regard the flow as laminar flow. A more applicable model is needed to calculate these areas appropriately. The  $k - \epsilon$  model is not a good model since for laminar flow since when  $k$  term reach zero, the destruction term will reach infinity. The equation is shown below:

$$\frac{\partial}{\partial x_j} (\rho \bar{U}_j \epsilon) = \frac{\partial}{\partial x_j} \left[ \left( \mu + \frac{\mu_t}{\sigma_\epsilon} \right) \frac{\partial \epsilon}{\partial x_i} \right] + \frac{\epsilon}{k} (c_{\epsilon 1} P_k - c_{\epsilon 2} \rho \epsilon) \quad (26)$$

If we use the  $k - \omega$  model which is developed by Wilcox, the problem will be solved, the  $k - \omega$  is shown below:

$$\frac{\partial}{\partial x_j} (\rho \bar{U}_j \omega) = \frac{\partial}{\partial x_j} \left[ \left( \mu + \frac{\mu_t}{\sigma_\omega} \right) \frac{\partial \omega}{\partial x_i} \right] + \frac{\omega}{k} (c_{\omega 1} P_k - c_{\omega 2} \rho \omega) \quad (27)$$

In the  $k - \omega$  model, if the term  $k$  goes to zero, other terms will still stay meaningful.

The production term is not included in the  $k - \omega$  model equation since:

$$\frac{\omega}{k} c_{\omega 1} P_k = \frac{\omega}{k} c_{\omega 1} \mu_t \left( \frac{\partial \bar{U}_i}{\partial x_j} + \frac{\partial \bar{U}_j}{\partial x_i} \right) \frac{\partial \bar{U}_i}{\partial x_j} = c_{\omega 1} c_\mu \left( \frac{\partial \bar{U}_i}{\partial x_j} + \frac{\partial \bar{U}_j}{\partial x_i} \right) \frac{\partial \bar{U}_i}{\partial x_j} \quad (28)$$

### 3.2 Ventilation Parameters

Ventilation effectiveness is a commonly used ventilation parameter which indicates the degree of effect for the influence of contaminant to the room. There are three ventilation effectiveness parameters; the first is the occupied zone ventilation effectiveness  $\epsilon_{OC}$ , the second is the local ventilation index  $\epsilon_P$  and the average ventilation effectiveness  $\langle \epsilon \rangle$ . The definition equation is shown in equation 22-24 [86].

$$\epsilon_{OC} = \frac{C_{out}}{C_{OC}} \quad (29)$$

$$\epsilon_P = \frac{C_{out}}{C_P} \quad (30)$$

$$\langle \epsilon \rangle = \frac{C_{out}}{\langle C \rangle} \quad (31)$$

$C_{OC}, C_P, \langle C \rangle, C_{out}$  mean the occupied one concentration, point P concentration, room mean concentration and outlet concentration respectively. The velocity should be simulated first in order to use CFD software to simulate the results of these parameters.

Contaminant source needs to be placed in the grid, then the Navier-Stokes equation is used to solve for  $C$ , which is equation 25.

$$\frac{\partial}{\partial x_j} (\rho \bar{U}_j C) = \frac{\partial}{\partial x_j} \left[ \left( \mu + \frac{\mu_t}{\sigma_c} \right) \frac{\partial C}{\partial x_j} \right] + S_P \quad (32)$$

The  $S_P$  in the equation means the contaminant volume in the grid. Since equation 25 is a linear equation, so the  $S_P$  will not change the parameter. The  $Pr$  number is usually constant ( $0.7 \leq \sigma_c \leq 0.9$ ). The  $C$  also have boundary condition which is  $C = 0$  at the inlet area and the concentration gradient is 0 when at the wall area ( $\partial C / \partial n = 0$ ) [86].

### **Local Age and Air Change Efficiency**

Local age means the time since a particular particle passed a designated point. The equation of local age is shown in equation 26.

$$\frac{\partial}{\partial x_j} (\rho \bar{U}_j \tau) = \frac{\partial}{\partial x_j} \left[ \left( \mu + \frac{\mu_t}{\sigma_\tau} \right) \frac{\partial \tau}{\partial x_j} \right] + \rho \quad (33)$$

$\sigma_\tau$  means the  $Pr$  number is usually constant ( $0.7 \leq \sigma_c \leq 0.9$ ).  $\tau$  also has a boundary condition of  $\tau = 0$  at the inlet region and does not have gradient.

There is an example to illustrate the local age prediction is shown in Figure 4. Moreover, the air change efficiency is defined as in equation 34.

$$\epsilon_a = \frac{\tau_n}{\langle \tau \rangle} \quad (34)$$

$\tau_n$  means the time constant which is defined as the volume of room  $V$  divided by the ventilation flow rate  $q$  which is shown in equation 29. And  $\langle \tau \rangle$  means the average local time in the room and figure 9 shows examples for local age prediction.

$$\tau_n = \frac{V}{q} \quad (35)$$

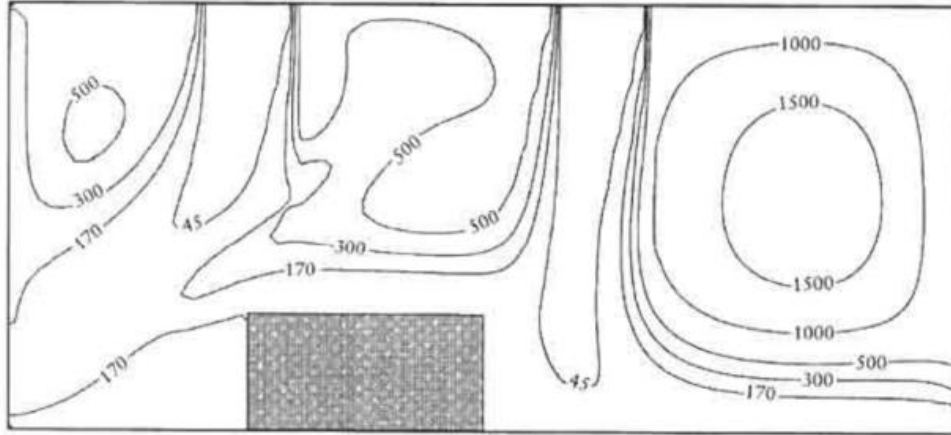


**Figure 9. Examples for local age prediction [86]**

### **Purging Flow Rate**

Table 4 shows examples for local age prediction. The local purging flow rate means the flow rate of the flow that leaves the outlet directly without returning to the point. To get the purging flow rate, we need to calculate the velocity field of the room. An example of the room configuration is shown in figure 4, and the simulated purging flow rate results are shown in Table 4. From the result, we can see that the  $U_p$  reach the maximum value in inlet area. This is because  $U_p$  is dependent on the flow condition as well as the area size. The reason area 1 has the lowest  $U_p$  is because the air is extracted by other outlets [86]. Figure 10 shows example for configuration of purging flow rate.

**Table 4. Examples for local age prediction [86]**

Area	$U_P(\text{m}^3/\text{h})$
1	281
2	294
3	289
4	372
5	432
6	385

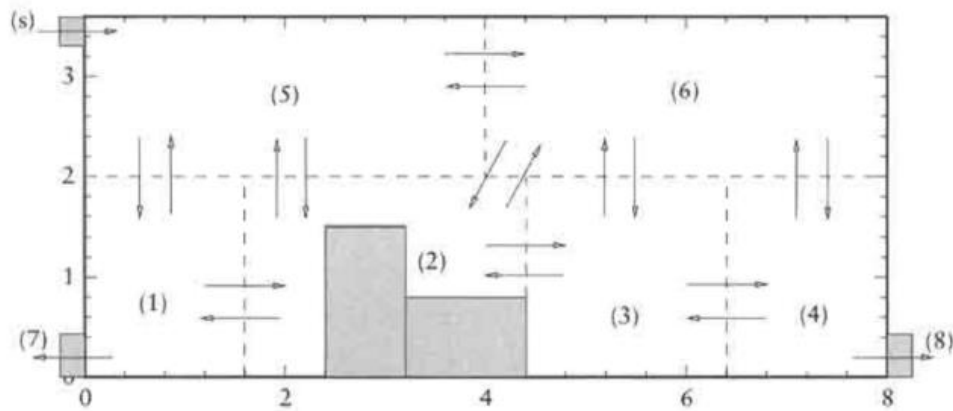


**Figure 10. Example for configuration of purging flow rate [86]**

### 3.3 Model Development and Set Up

#### 3.3.1 Geometry

The size of the general workshop, inlet, outlet, and contaminant source is shown in Table 5. The computational geometries are illustrated in Table 6, in this thesis, seven different ventilation system installation setting has been proposed. The setting of different installation schemes is also shown in Table 6.

Scheme 3 is shown in Figure 13; the outlet is located at the top far side of the workshop. Scheme 4 is shown in Figure 14; the outlet setting is as same as scheme 1, there is an additional inlet at the inlet side.

**Table 5. Example for configuration of purging flow rate [86]**

<b>Workshop</b>	
Length	10 m
Width	10 m
Height	5 m
<b>Air Inlet</b>	
Diameter	1 m
<b>Air Outlet</b>	
Edge length	1 m
<b>Contaminant Source</b>	
Diameter	0.5 m

**Table 6. Computational geometry of installation schemes**

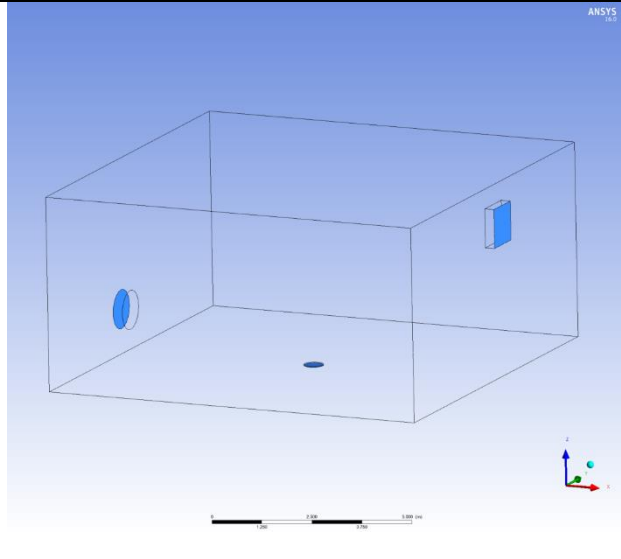
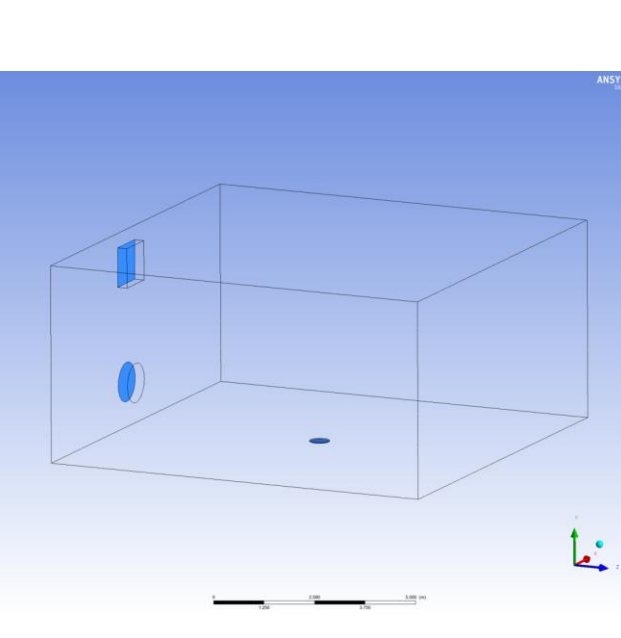
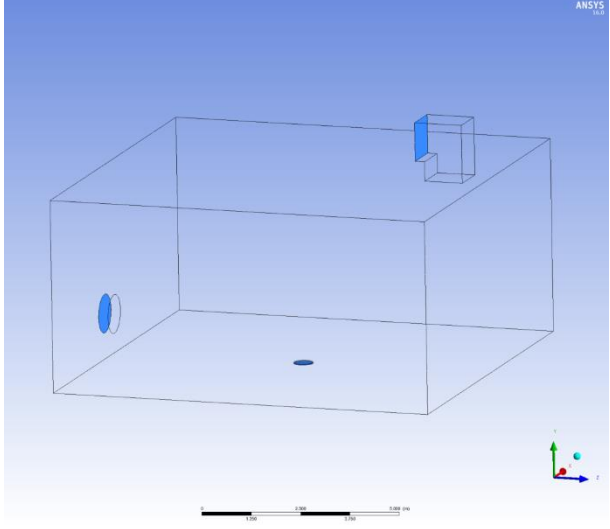
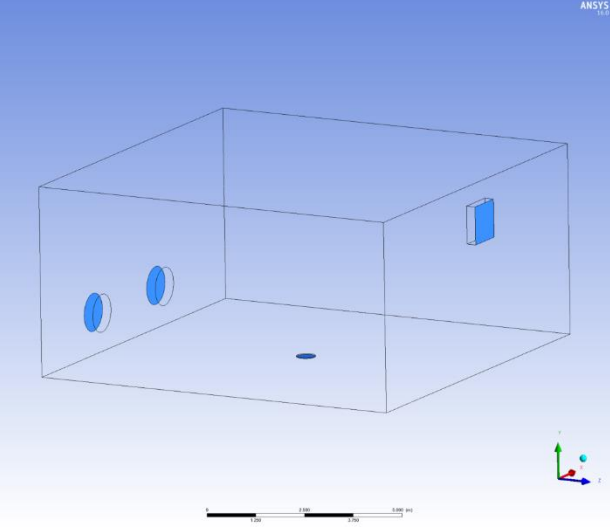
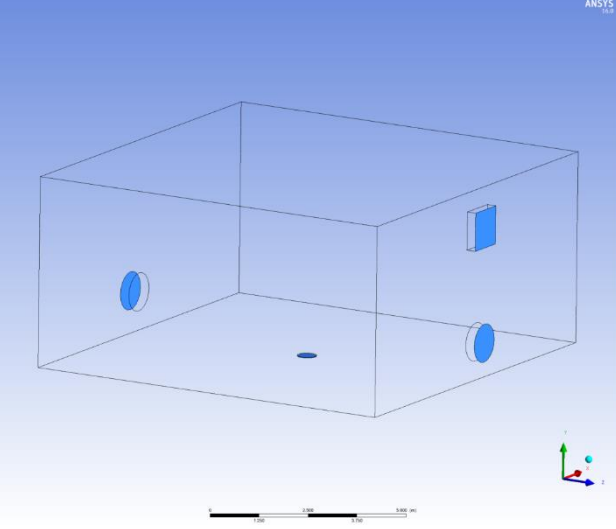
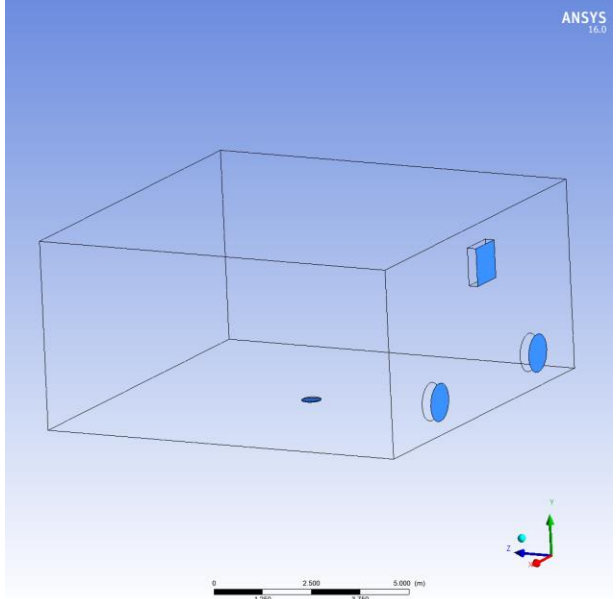
<b>Scheme</b>	<b>Geometry Illustration</b>	<b>Inlet and Outlet Arrangement</b>
1	 A 3D perspective view of a rectangular box. On the left vertical face, there is a blue circular inlet. On the right vertical face, there is a blue rectangular outlet. The bottom surface has a small blue oval. A coordinate system with x, y, and z axes is shown in the bottom right corner. A scale bar at the bottom indicates dimensions of 1,000, 2,000, and 3,000 mm. The ANSYS logo is in the top right corner.	Outlet is on the opposite side of inlet
2	 A 3D perspective view of a rectangular box. On the left vertical face, there is a blue circular inlet. On the top horizontal face, there is a blue rectangular outlet. The bottom surface has a small blue oval. A coordinate system with x, y, and z axes is shown in the bottom right corner. A scale bar at the bottom indicates dimensions of 1,000, 2,000, and 3,000 mm. The ANSYS logo is in the top right corner.	Airflow inlet located on the same side as an outlet.

Table 6 Continued

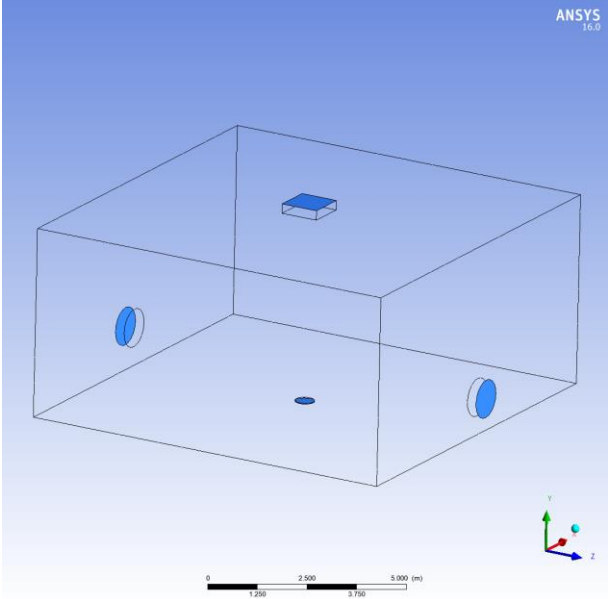
Scheme	Geometry Illustration	Inlet and Outlet Arrangement
3	 <p>The illustration shows a 3D wireframe model of a rectangular workshop. A blue circular inlet is located on the left wall. A blue rectangular outlet is located on the top far side wall. A coordinate system with x, y, and z axes is shown in the bottom right corner. A scale bar at the bottom indicates dimensions of 0, 1.500, 3.000, and 4.500 meters. The ANSYS 16.2 logo is in the top right corner.</p>	<p>Outlet is located at the top far side of the workshop</p>
4	 <p>The illustration shows a 3D wireframe model of a rectangular workshop. Two blue circular inlets are located on the left wall. A blue rectangular outlet is located on the right wall. A coordinate system with x, y, and z axes is shown in the bottom right corner. A scale bar at the bottom indicates dimensions of 0, 1.500, 3.000, and 4.500 meters. The ANSYS 16.2 logo is in the top right corner.</p>	<p>Outlet setting is as same as scheme 1; there is an additional inlet at the inlet side.</p>



**Table 6 Continued**

Scheme	Geometry Illustration	Inlet and Outlet Arrangement
5		<p>Outlet setting is as same as scheme 2; there is an additional inlet at opposite side of the inlet.</p>
6		<p>Outlet setting is as same as scheme 2; there is an additional inlet at the same side of the inlet.</p>

**Table 6 Continued**

Scheme	Geometry Illustration	Inlet and Outlet Arrangement
7		<p>Outlet setting is as same as scheme 5; the outlet is located at the top center.</p>

### 3.3.2 Mesh

The meshing of the computational geometry is completed in ANSYS meshing tools. The computational grid of different schemes is shown in Table 7. The inflation of boundary layers technique was used to make high-quality and high-resolution computational grid. The resolution of areas where the velocity gradient is high was refined. Four level of grids were constructed based on different resolution. The total number of cells of different schemes are shown in Table 7. The fine grid of scheme 1 which has 217,018 cells is shown in Figure 11.

**Table 7. Cell data of different schemes based on different level of mesh quality**

Scheme	Coarse Grid	Medium Grid	Fine Grid	Finest Grid
1	31,306	74,333	217,018	572,880
2	30,986	77,438	226,001	573,267
3	30,561	74,167	211,118	578,527
4	37,891	78,451	21,9139	57,5278
5	37,553	78,733	217,873	575,124
6	37,933	79,788	227,049	574,720
7	38,760	78,548	219,607	575,092

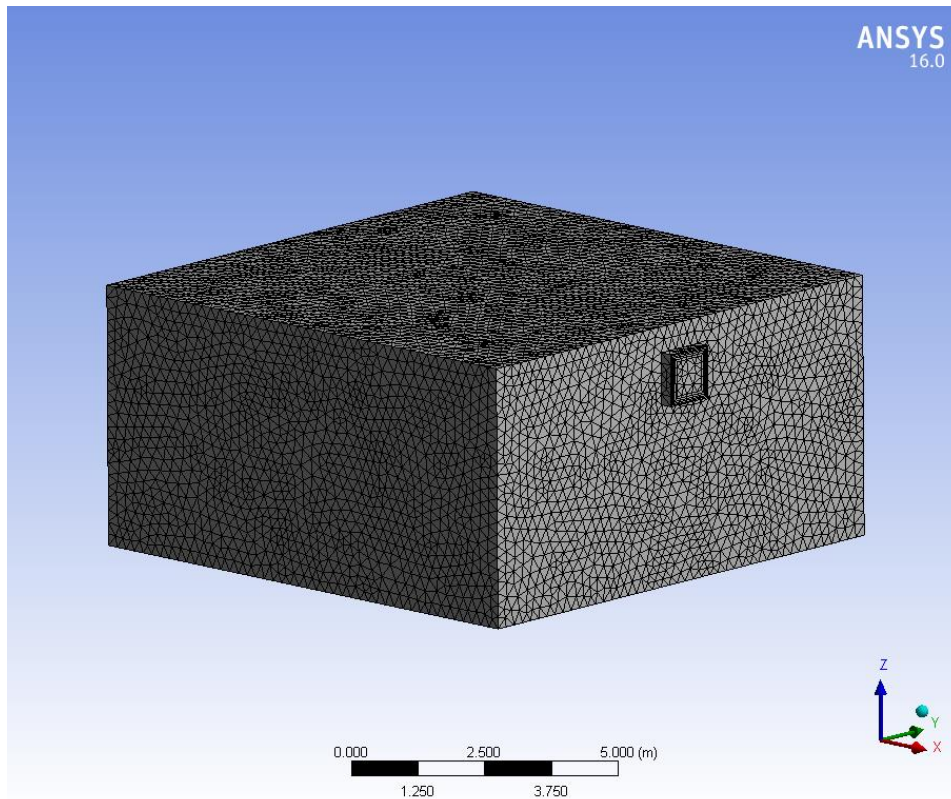


**Figure 11. Fine computational grid of scheme 1**

### 3.3.3 Boundary Conditions

The boundary conditions were chosen to replicate the typical dilution ventilation system. The workshop surfaces were set as smooth no-slip walls. The outlet of the ventilation system was set to outlet vent which has -100 Pascal pressure difference and the backflow direction was specified as normal to the boundary, which was based on the Reynolds number at the actual ventilation inlet. The inlet of the ventilation system was set to inlet vent with zero static pressure difference since the exhaust fan is located at the outlet. The contaminant source is set to mass flow inlet, the mass flow rate of the source is 0.5 kg/s. In this thesis, hydrogen sulfide is used as the sample contaminant materials to demonstrate the concentration distribution in the workshop, which can evaluate the performance of different installation schemes.

### 3.3.4 Solver Settings

3D steady-state simulations were conducted using ANSYS Fluent. Two equations realizable k- $\epsilon$  viscous model was used to calculate the airflow behavior in this thesis, using constants setting of this model as shown in Table 8. Standard wall functions are used for simulation of results of the near-wall area. Pressure-velocity coupling was solved by the SIMPLE algorithm, pressure interpolation is second order, and first-order upwind discretization schemes were used for turbulent kinetic energy term and turbulent dissipation rate term. Second-order upwind discretization schemes were used in momentum, air, and energy terms. Convergence of the solution was monitored carefully. In most simulation cases, oscillatory convergence was present. The hybrid initialization method is used to initialize the solution, and the interval of iterations was set to 1,000 which is an average iteration time that the solution can be converged.

**Table 8. Constants setting of two equations realizable k- $\epsilon$  viscous model**

<b>Constant</b>	<b>Value</b>
C2-Epsilon	1.9
TKE Prandtl Number	1
TDR Prandtl Number	1.2
Energy Prandtl Number	0.85
Wall Prandtl Number	0.85
Turbulent Schmidt Number	0.7

## 4. RESULTS AND DISCUSSION

### 4.1 Grid Independence Analysis

Grid independence analysis is important to get accurate results since a coarse grid can significantly impact the simulation results. However, an over-detailed mesh will increase the calculation load significantly. A grid independency analysis is necessary to obtain an appropriate reference meshing quality with results that are grid independent. The geometry and meshing data of nine installation schemes are not changing significantly. Scheme 1 is used as a reference case to conduct grid independency analysis. The total number of 4 different meshing quality was used in the independence analysis, the cell data was stated in part three: (1) coarse grid; 31,306 cells; (2) medium grid; 74,333 cells; (3) fine grid; 217,018 cells; (4) finest grid; 572,880 cells. The grids are compared based on the velocity contour of the cross-section between inlet and outlet, which is shown in Figure 12-15.

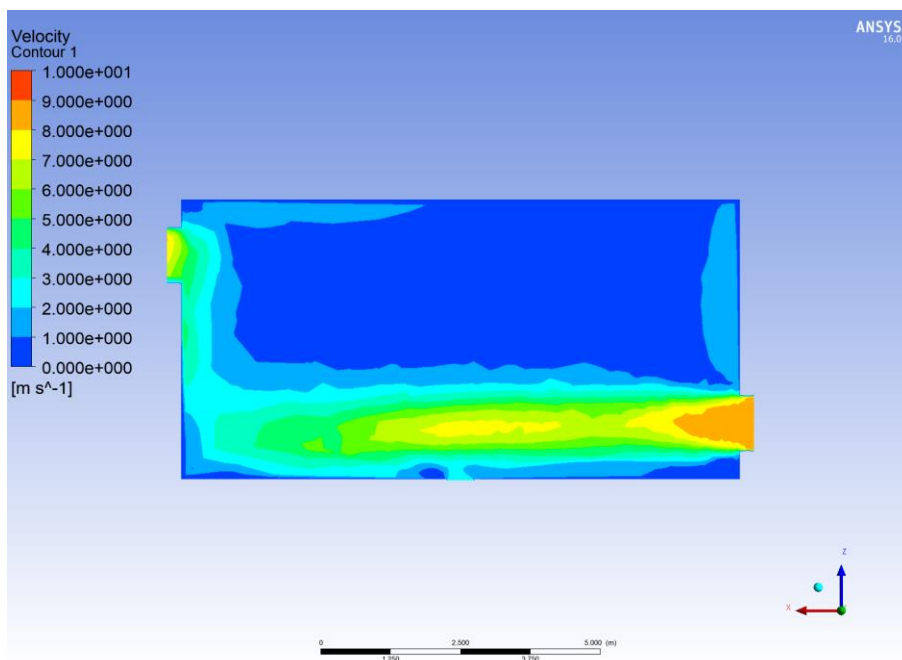


**Figure 12. Velocity contour of coarse-meshed scheme one geometry**

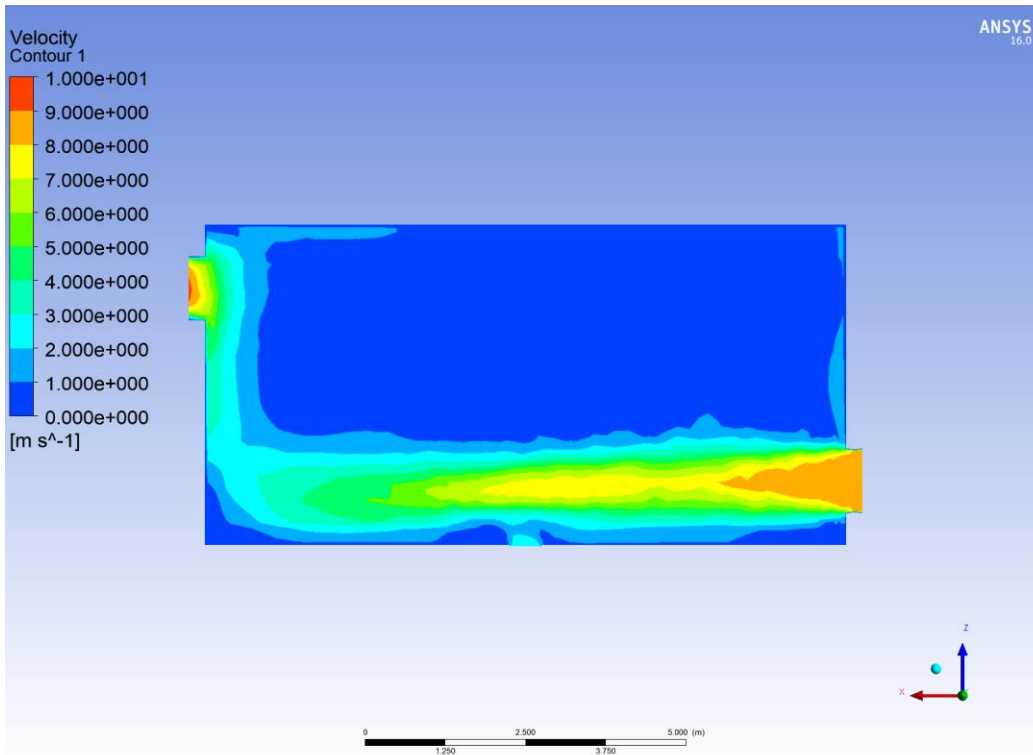


**Figure 13. Velocity contour of medium-meshed scheme 1 geometry**

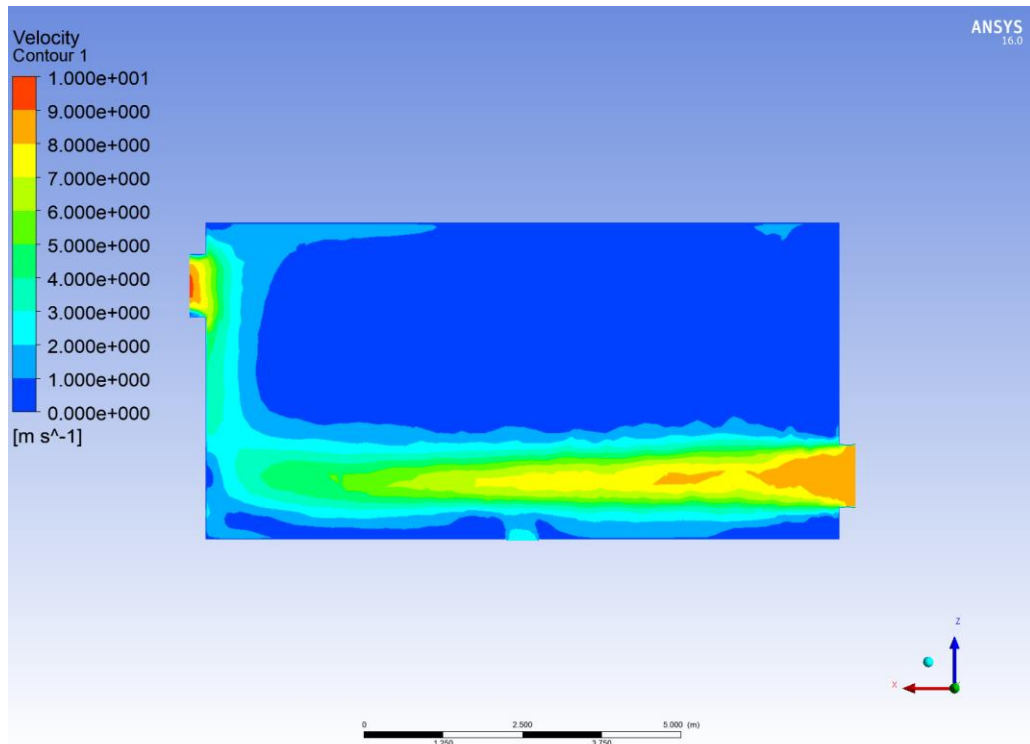


**Figure 14. Velocity contour of fine-meshed scheme 1 geometry**

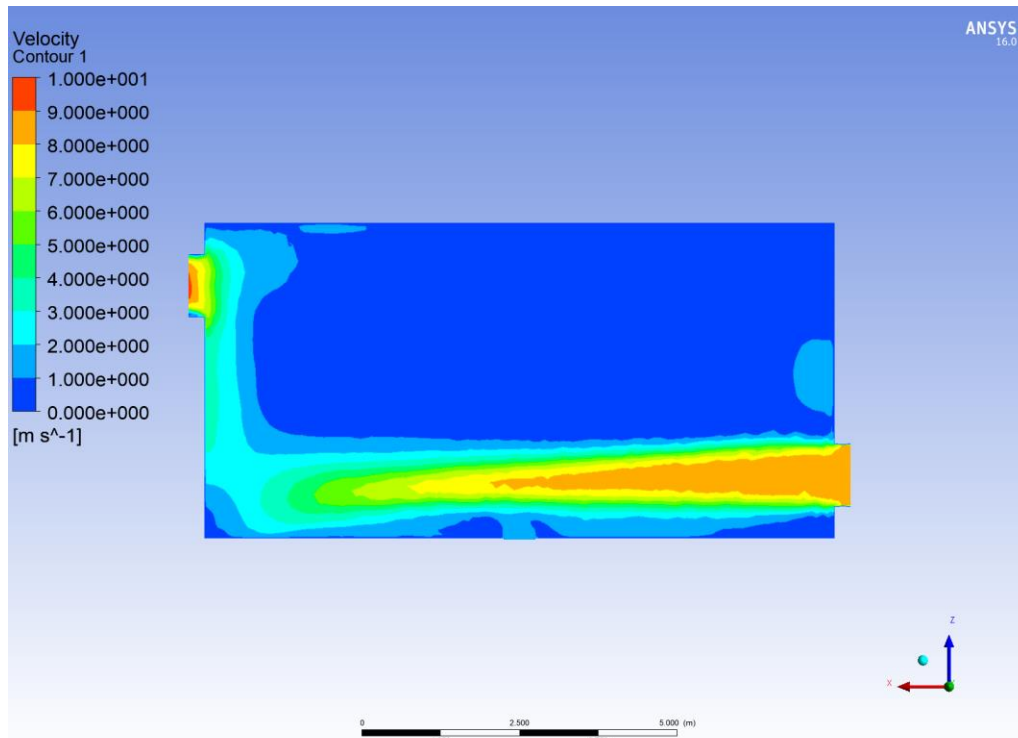


**Figure 15. Velocity contour of finest meshed scheme 1 geometry**

From grid independency analysis, it is concluded that the fine grid provides satisfying grid independency so the fine meshing quality will be used for further simulation and evaluation.

#### 4.2 Ventilation Performance Analysis of Single-inlet Installation Schemes

The velocity contour at the cross-section between inlet and outlet of scheme 1-3 are shown in Figure 16-18. As can be seen from the figures, in the single inlet schemes, the air flow in the middle of the workshop is relatively high and fully developed. However, as the outlet geometry of scheme 3 is not conducive to the full development of the airflow, the air velocity of the third scheme in the middle of the workshop is obviously lower than scheme 1 and scheme 2, which shows that the outlet arrangement of scheme 3 cannot improve the ventilation efficiency of confined workshop.



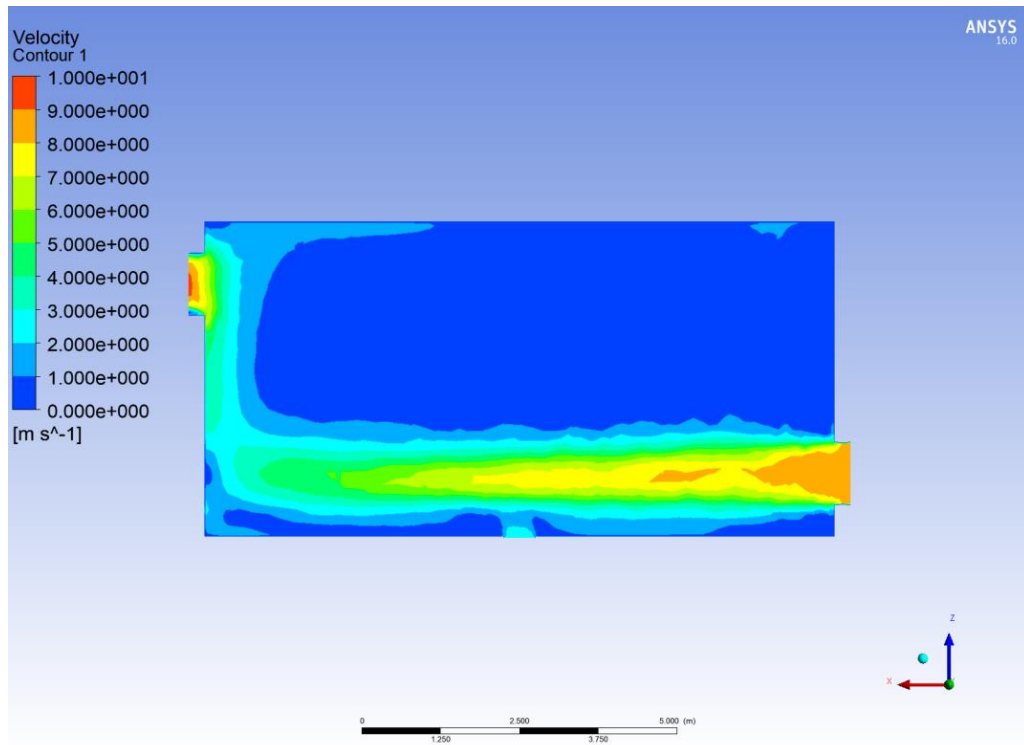


**Figure 16. Velocity contour of scheme 1 (cross section between inlet and outlet)**

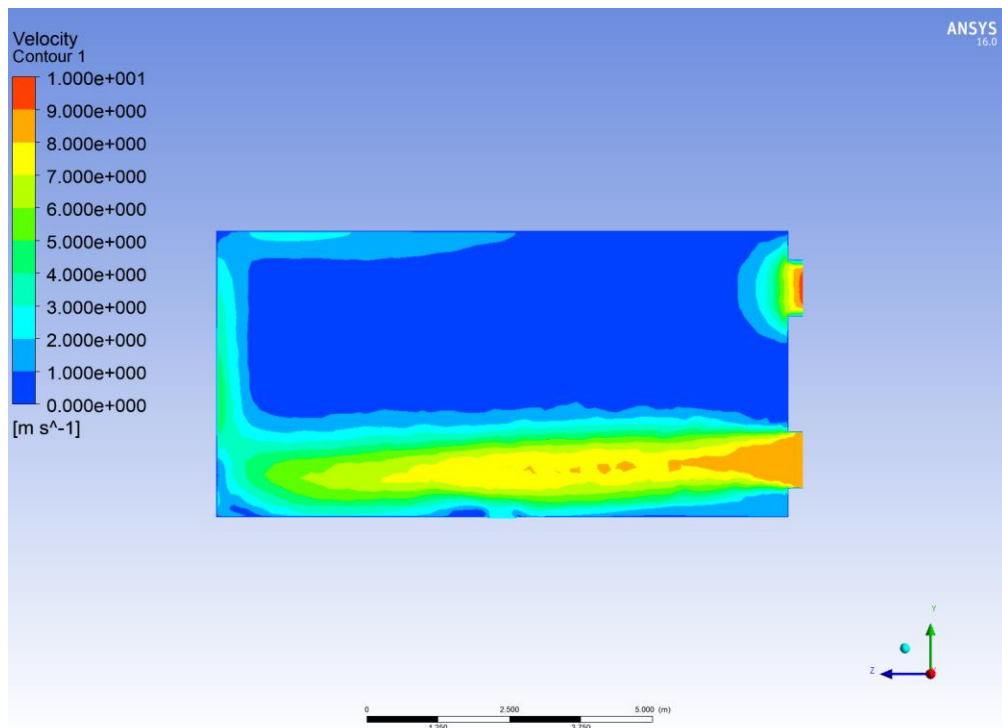


**Figure 17. Velocity contour of scheme 2 (cross section between inlet and outlet)**

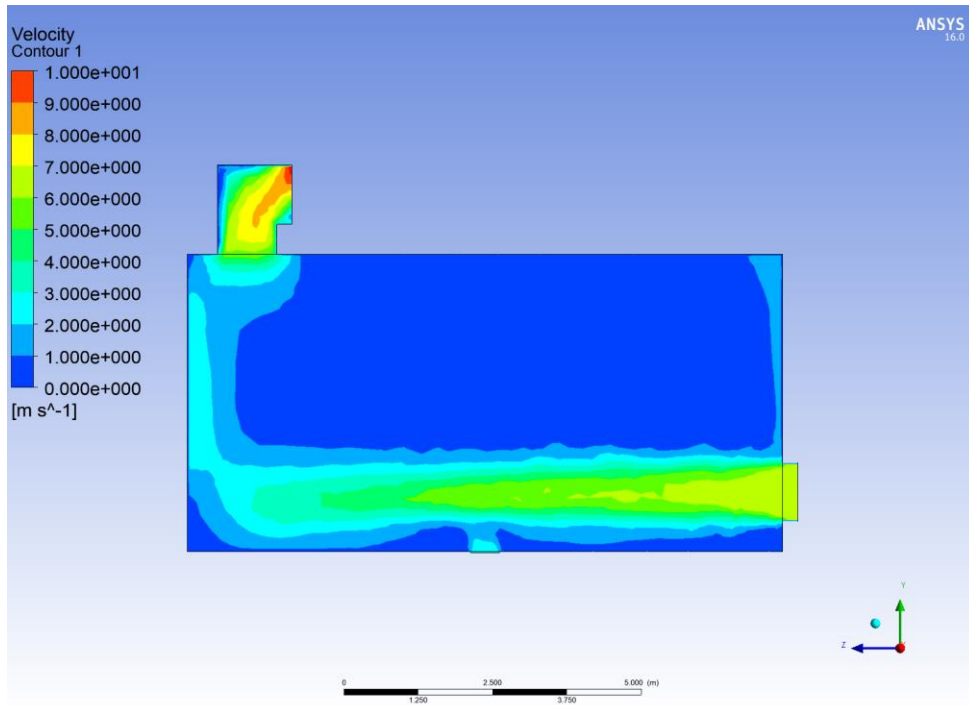


**Figure 18. Velocity contour of scheme 3 (cross section between inlet and outlet)**

The cross-section velocity contour at the height of 1 meter of scheme 1-3 is shown in Figure 19-21. It can be seen from the Figures that the airflow in scheme 1 can cover a larger area horizontally and the coverage of Scheme 2 is relatively satisfying. However, in Scheme 3, due to the airflow velocity decreases caused by the arrangement of the outlets. Although the coverage ranges of scheme 3 are the same as the first two schemes, the lower wind speed will adversely affect the ventilation efficiency.

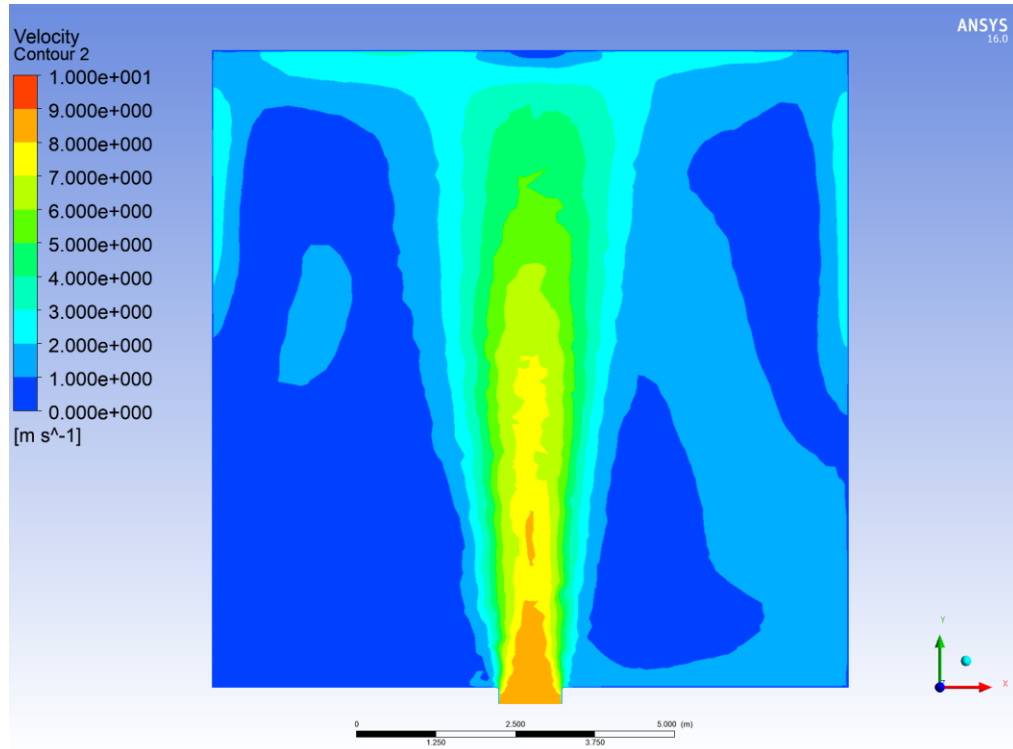


**Figure 19. Velocity contour of scheme 1 (Cross section at the height of 1 meter)**

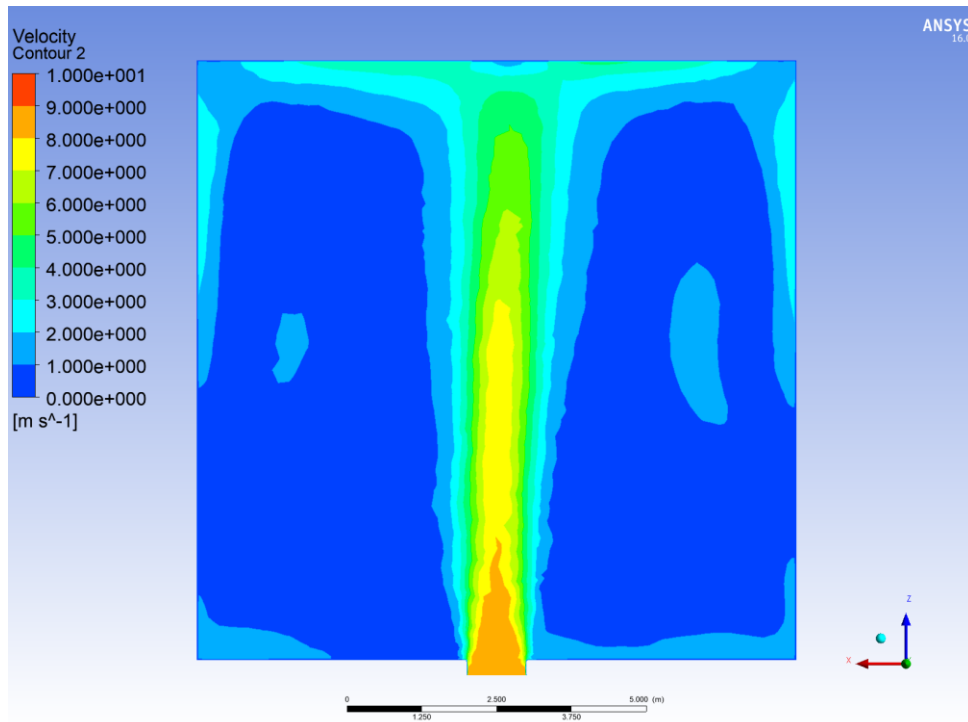


**Figure 20. Velocity contour of scheme 2 (cross section at the height of 1 meter)**

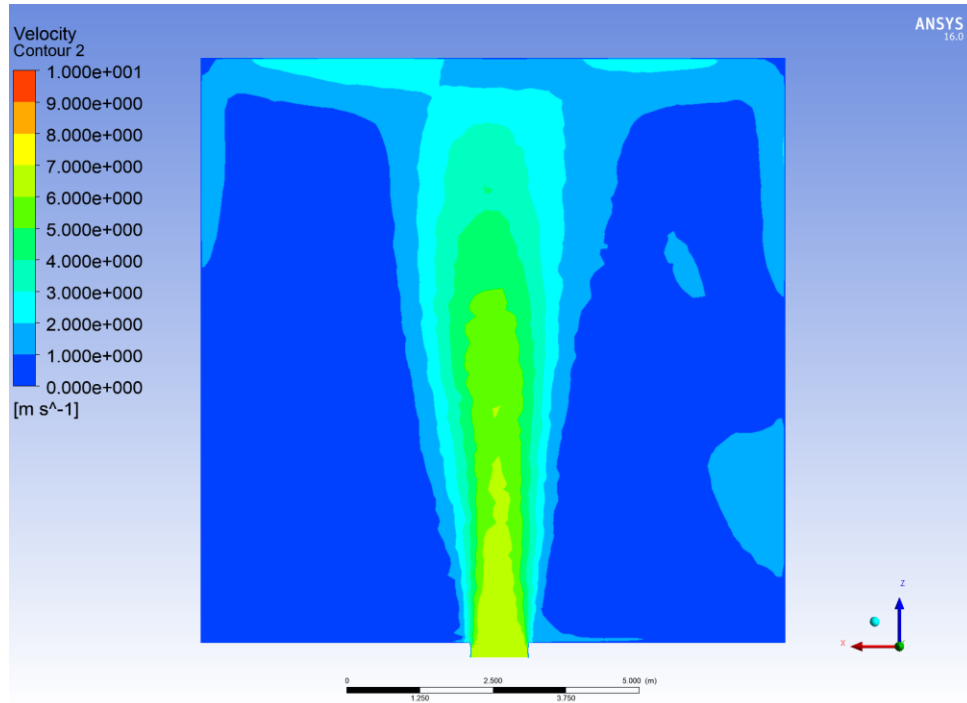


**Figure 21. Velocity contour of scheme 3 (cross section at the height of 1 meter)**

The carbon monoxide mass fraction contour at the cross-section between the inlet and outlet of scheme 1-3 are shown in Figure 22-24. As can be seen from the Figures, the carbon monoxide removal efficiency of the scheme 2 is slightly better than that of the first scheme 1. The geometry setting of scheme 3 leads to a reduction of the air velocity, so the carbon monoxide removal efficiency of scheme 1 and scheme 2 are better than the scheme 3.

However, it can also be seen from the figures that although the airflow of the three schemes has been fully developed at the source of pollution, the concentrations of carbon monoxide in downwind have risen significantly, which would be extremely detrimental to the health of workers working in that area. This shortcoming is the biggest problem with a single-inlet ventilation system.

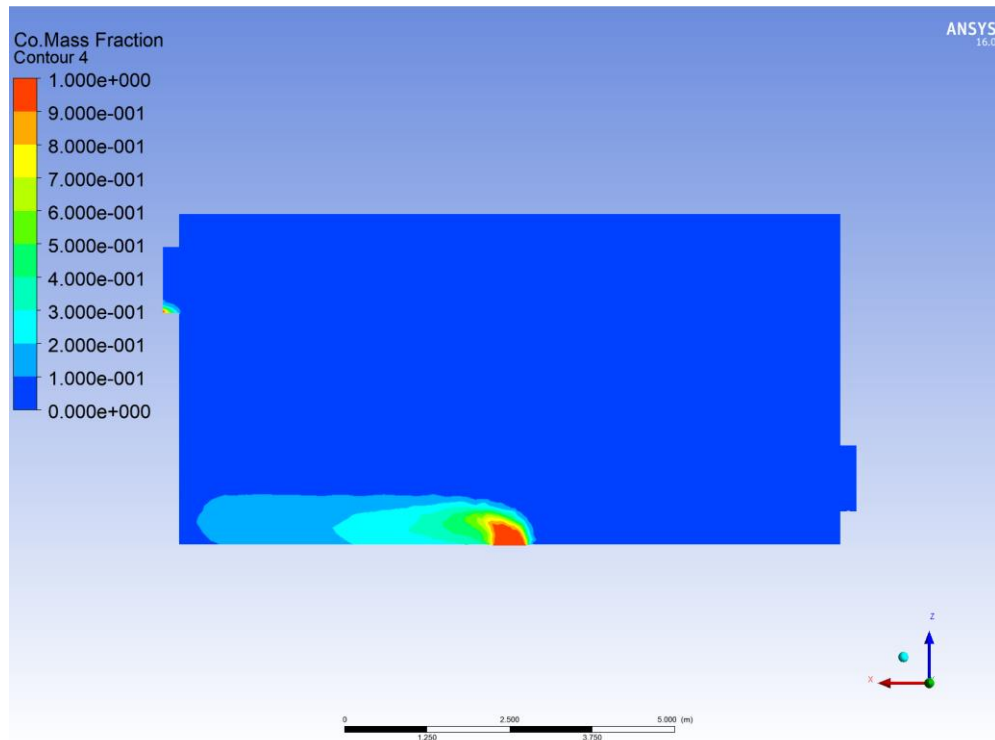


**Figure 22. Carbon monoxide mass fraction contour of scheme 1 (cross section between inlet and outlet)**

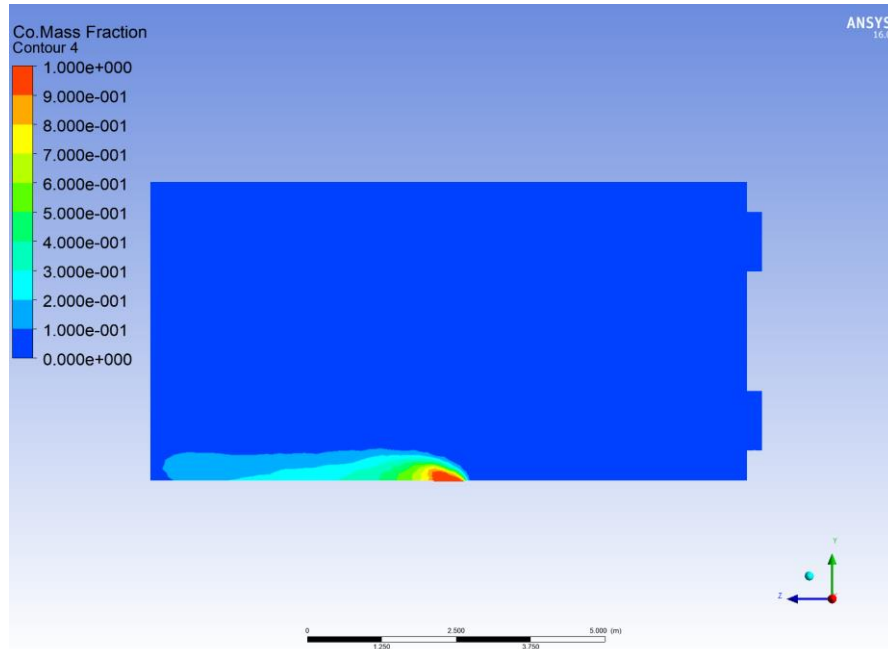


**Figure 23. Carbon monoxide mass fraction contour of scheme 2 (cross section between inlet and outlet)**

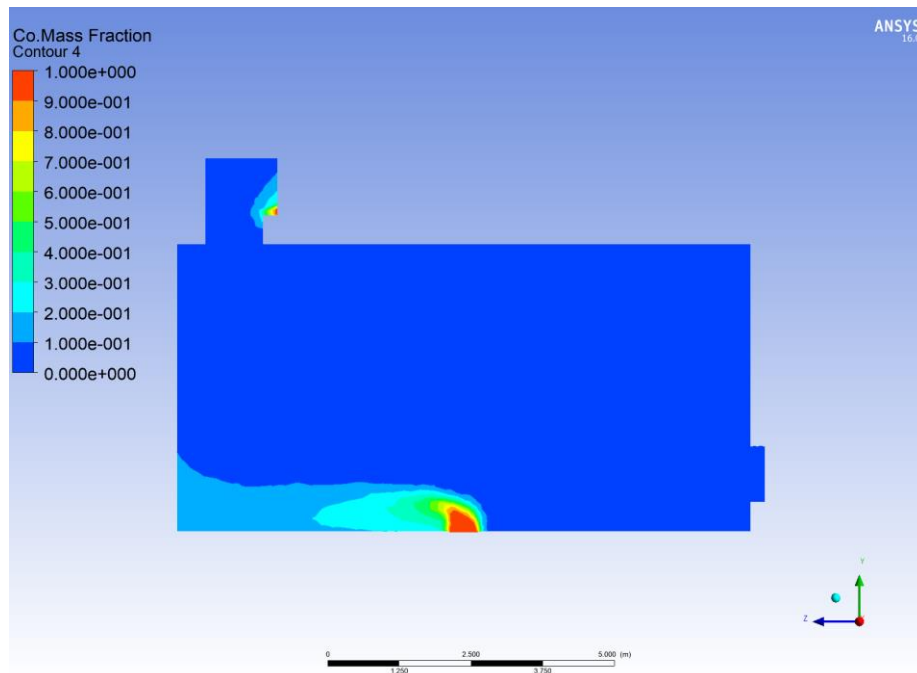


**Figure 24. Carbon monoxide mass fraction contour of scheme 3 (cross section between inlet and outlet)**

### 4.3 Ventilation Performance Analysis of Two-inlet Installation Schemes

The velocity contour at the cross-section between inlet and outlet of scheme 4-7 are shown in Figure 25-28. As can be seen from the figures, the airflow velocity of scheme 4 and scheme 6 in the middle of the workshop is very low since the air inlets are located on far sides. Meanwhile, the airflow velocity of scheme 5 and scheme 7 are preferable in the central part of the plant. Due to the additional air inlets, the airflow velocity is slightly reduced. However, the airflow velocity of scheme 5 and scheme 7 are distributed more uniform and symmetric than the single-inlet schemes.

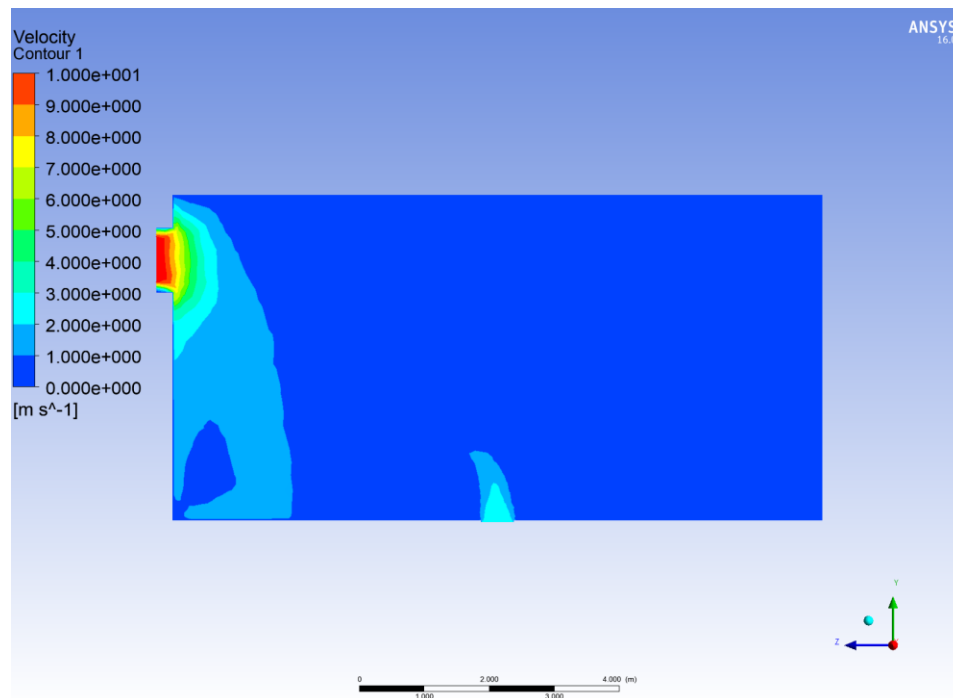


**Figure 25. Velocity contour of scheme 4 (cross section between inlet and outlet)**

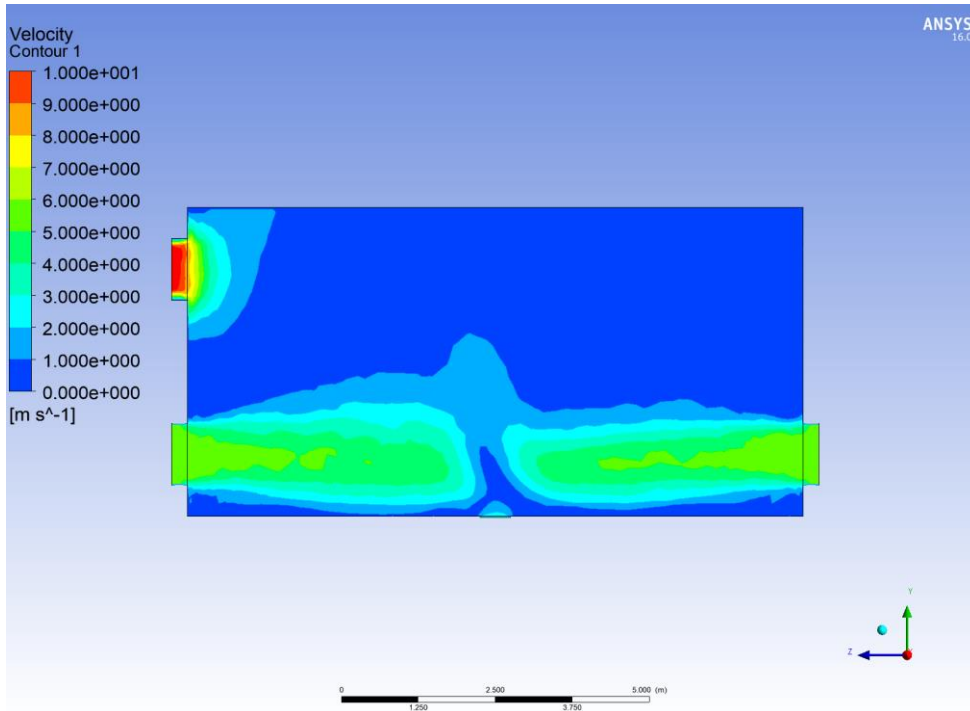


**Figure 26. Velocity contour of scheme 5 (cross section between inlet and outlet)**

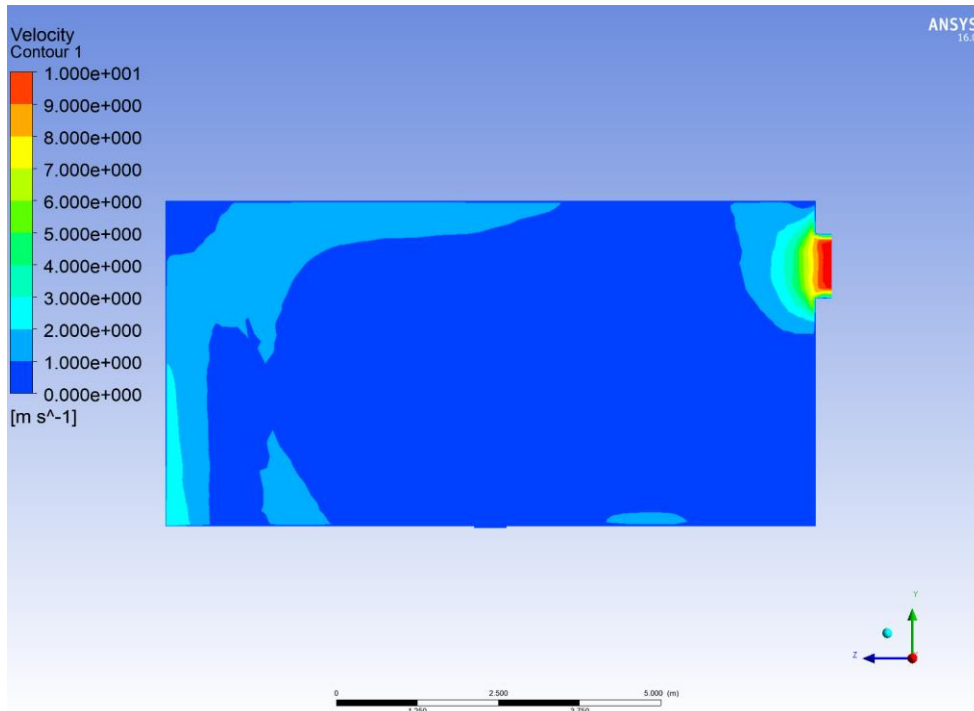


**Figure 27. Velocity contour of scheme 6 (cross section between inlet and outlet)**



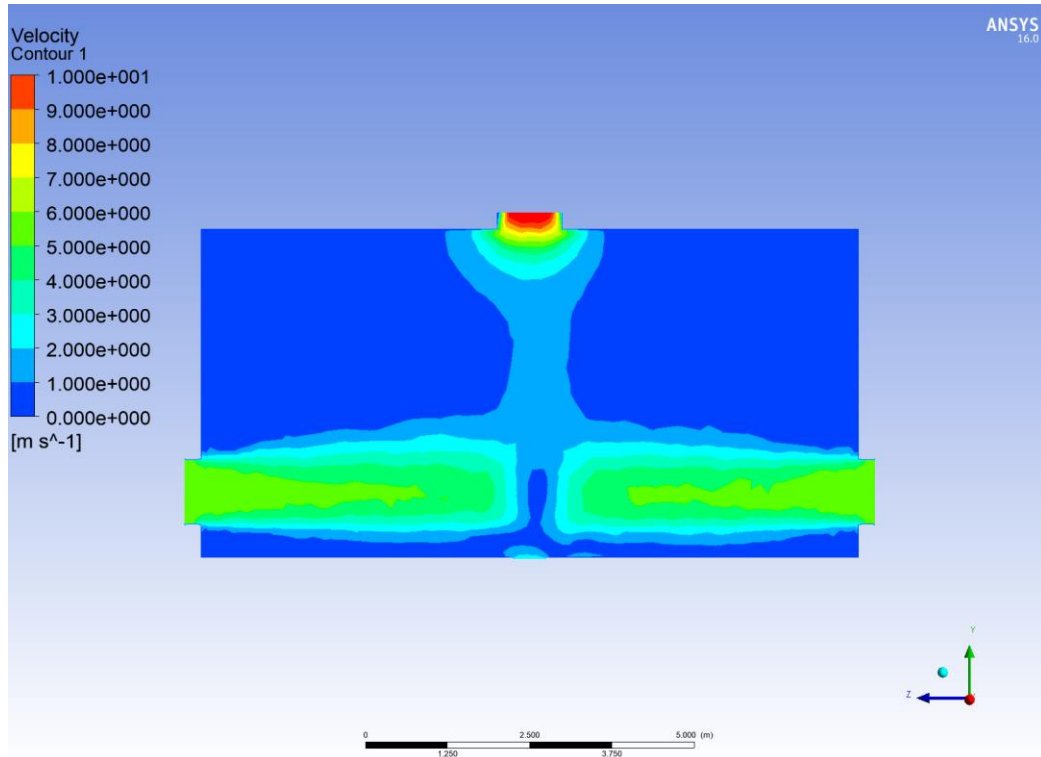


**Figure 28. Velocity contour of scheme 7 (cross section between inlet and outlet)**

The cross-section velocity contour at height of 1 meter of scheme 4-7 are shown in Figure 29-32. It can be seen from the figures that the air velocity develops better in the horizontal direction and covers a wider area than single-inlet ventilation system scheme 4 and scheme 6 due to its additional airflow inlet. The coverage of scheme 5 and scheme 7 are reduced since the relatively reduced airflow, but coverage is better in the middle of the plant.

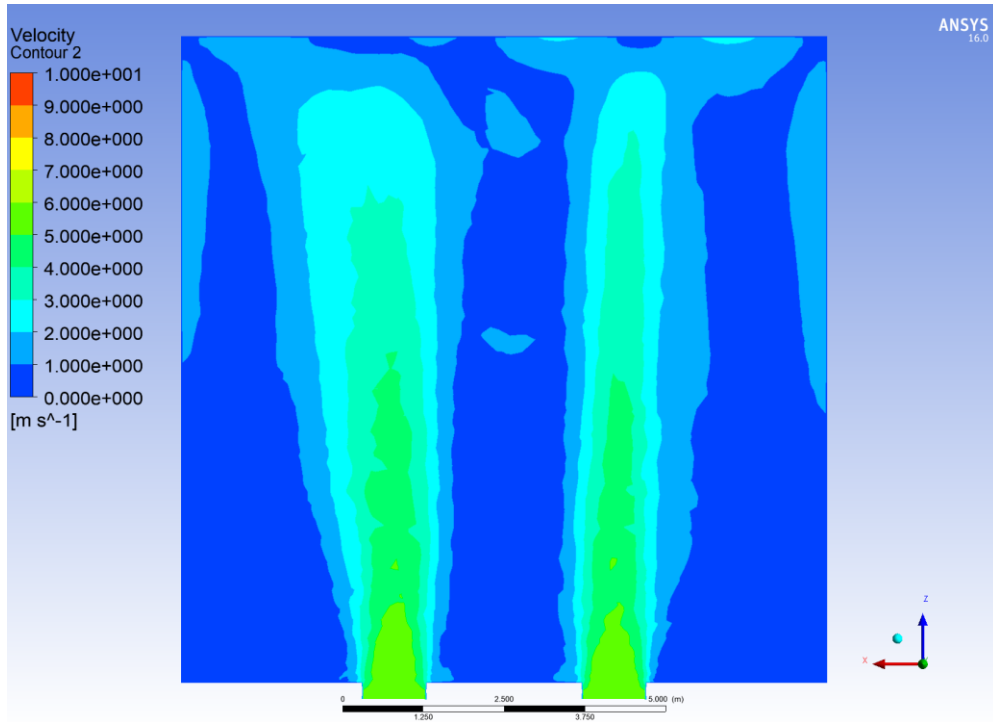


**Figure 29. Velocity contour of scheme 4 (cross section at height of 1 meter)**

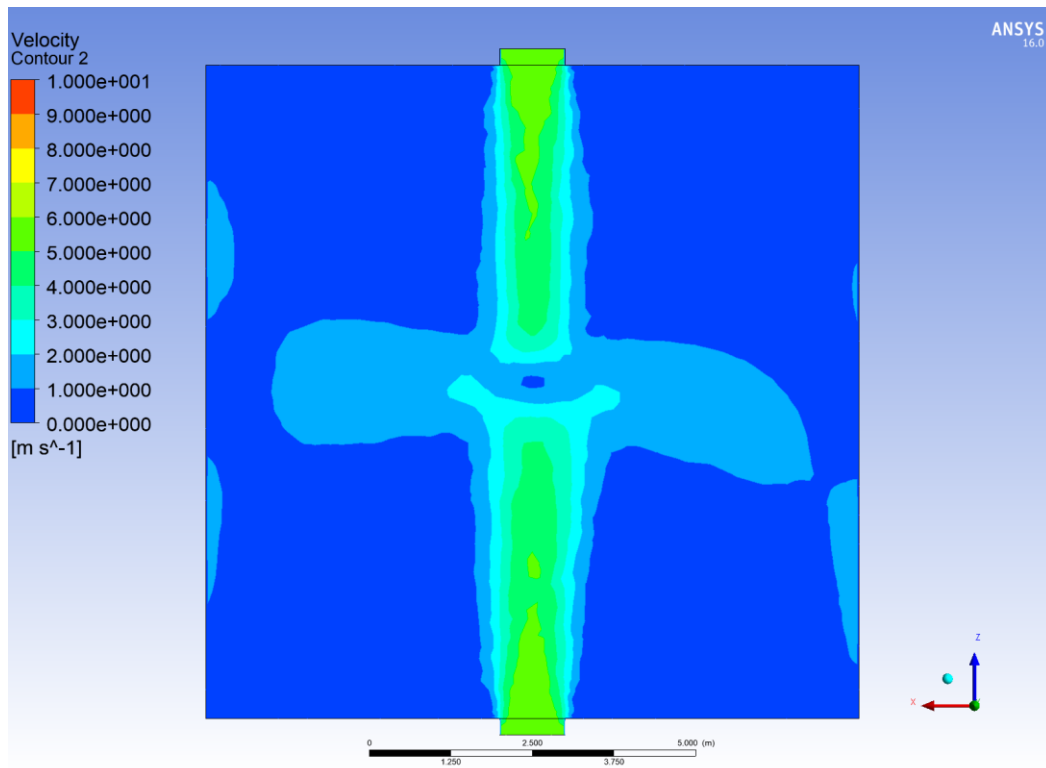


**Figure 30. Velocity contour of scheme 5 (cross section at height of 1 meter)**

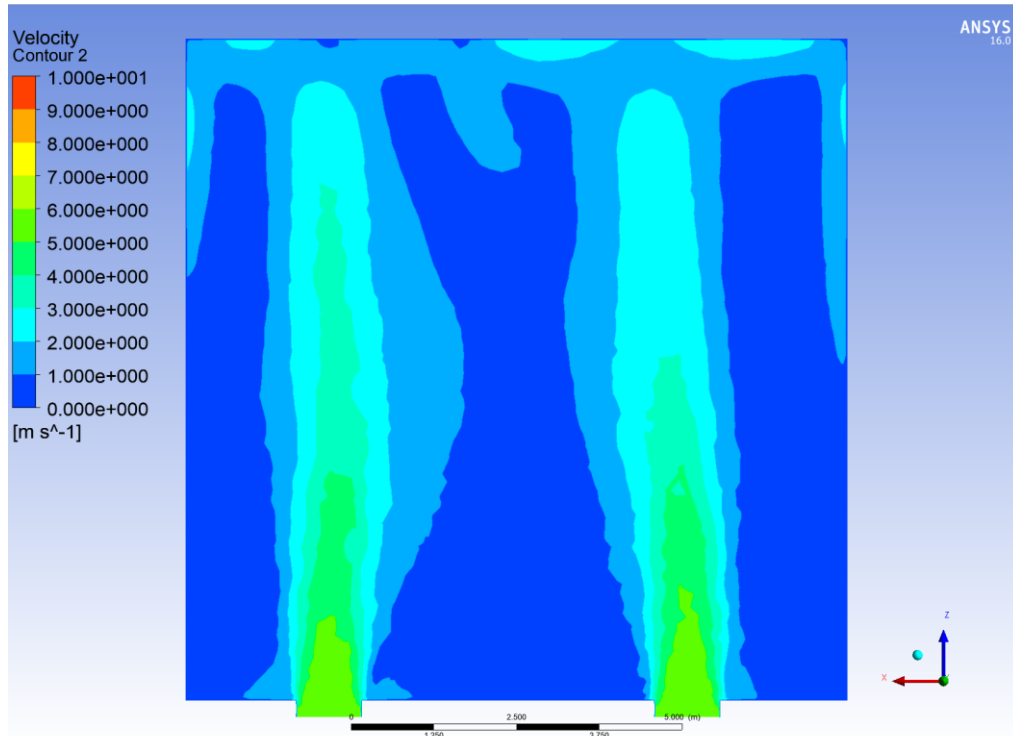


**Figure 31. Velocity contour of scheme 6 (cross section at height of 1 meter)**

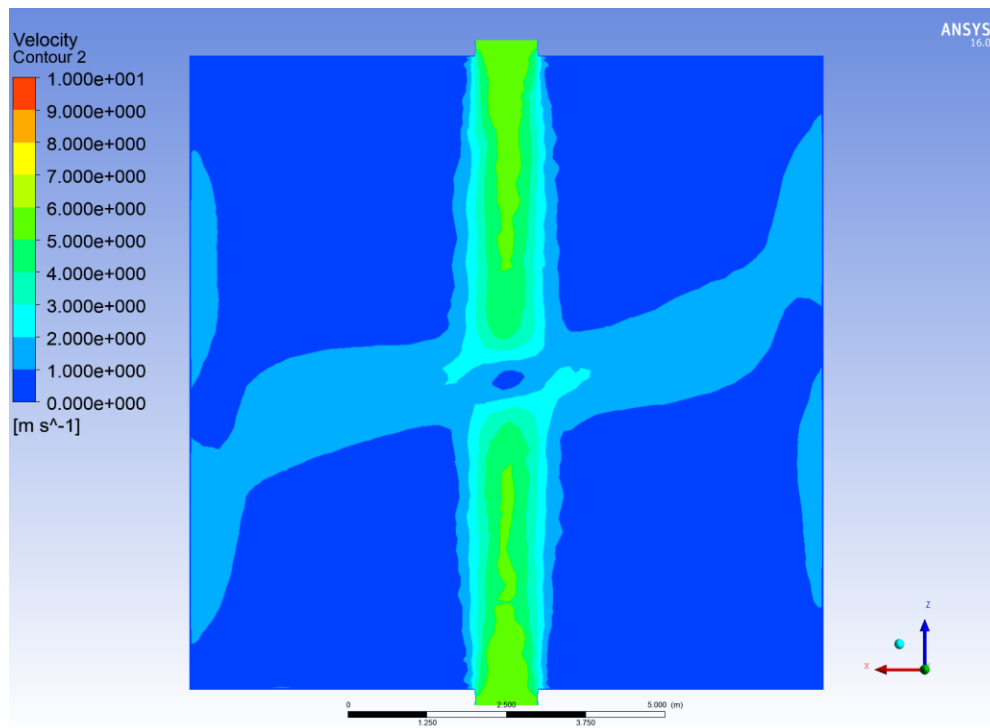


**Figure 32. Velocity contour of scheme 6 (cross section at height of 1 meter)**

The carbon monoxide mass fraction contour at the cross-section between inlet and outlet of scheme 4-7 are shown in Figures 33-36. Due to scheme 4's poor coverage in the middle of workshop, its carbon monoxide removal efficiency is greatly reduced. In the case when there is a source of contamination in the center of the plant, its removal efficiency is even lower than that of all single-inlet schemes.

However, the carbon monoxide removal efficiency of scheme 6 is significantly higher than that of scheme 4 because the airflow velocity of the scheme is more fully developed and covers the middle of the workshop while ensuring coverage of marginal areas. Therefore, the carbon monoxide removal efficiency of scheme 6 when contaminant source located at the center is significantly better than single-inlet schemes.

The removal of carbon monoxide is most effective for scheme 5 and 7 because the contaminant source is located at the center of the workshop and the location of the inlets are at the middle of the plant which allows the ventilation system to adequately controlled the source. Besides, since the outlets are symmetrically placed, the concentration of carbon monoxide will not rise at the downwind areas which solves the biggest problem for the single-inlet schemes.

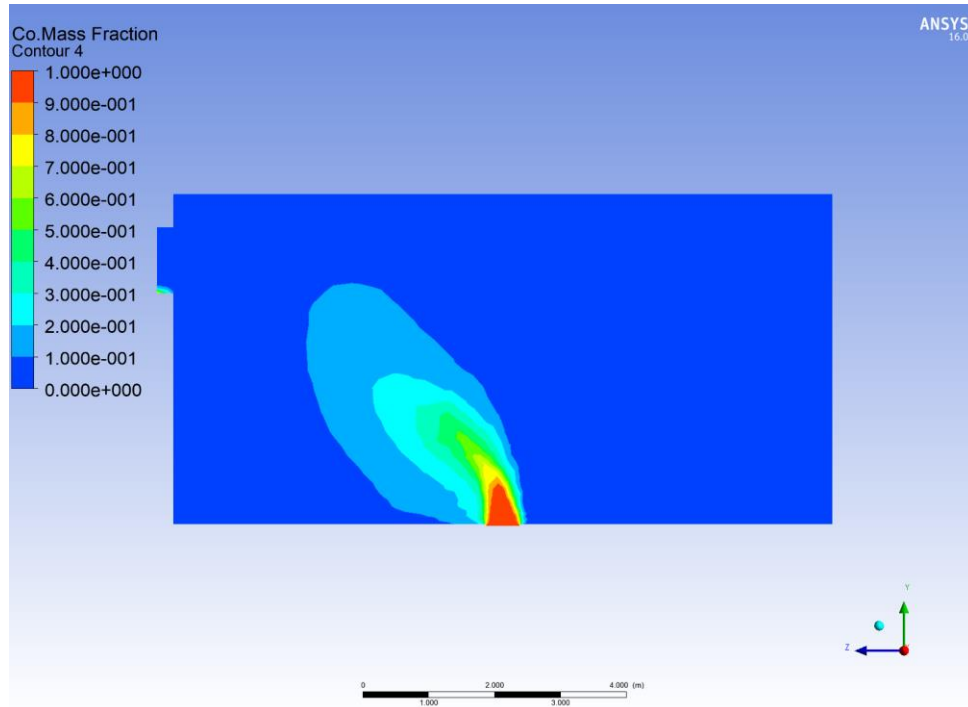


**Figure 33. Carbon monoxide mass fraction contour of scheme 4 (cross section between inlet and outlet)**

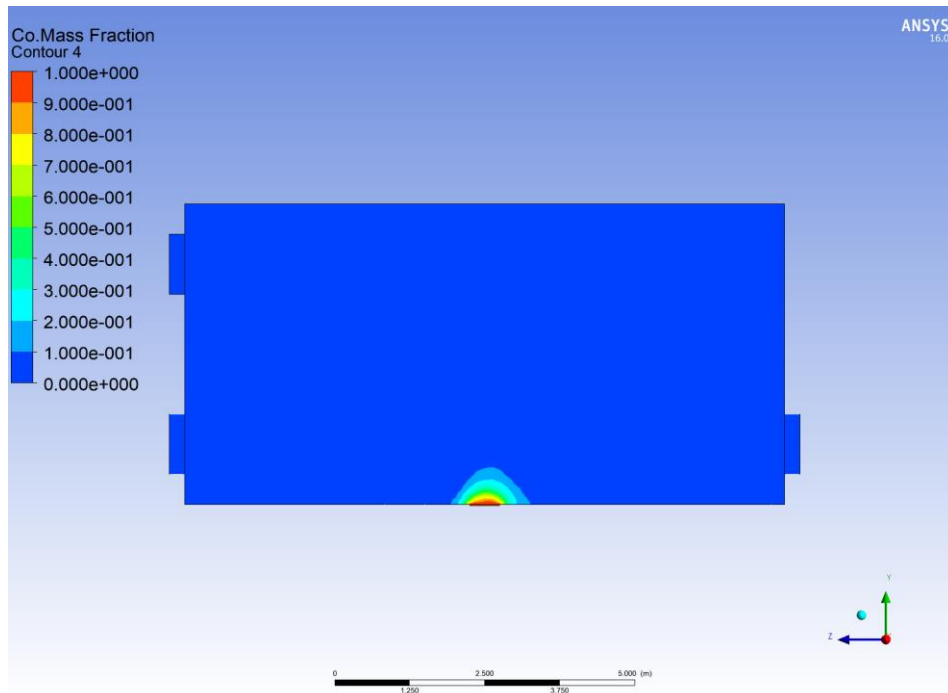


**Figure 34. Carbon monoxide mass fraction contour of scheme 5 (cross section between inlet and outlet)**

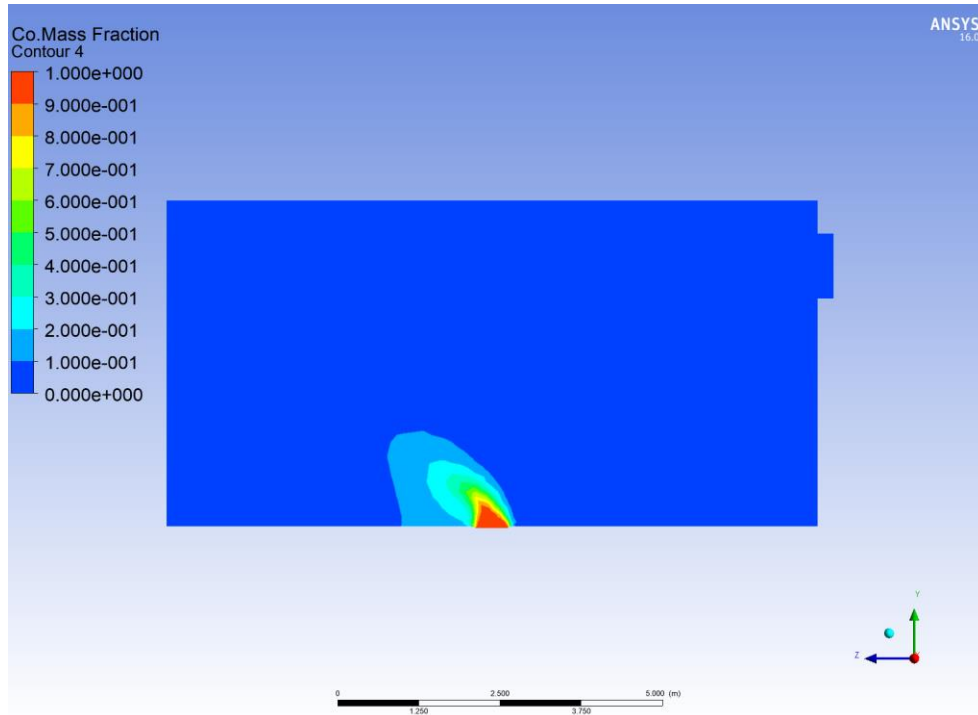


**Figure 35. Carbon monoxide mass fraction contour of scheme 4 (cross section between inlet and outlet)**

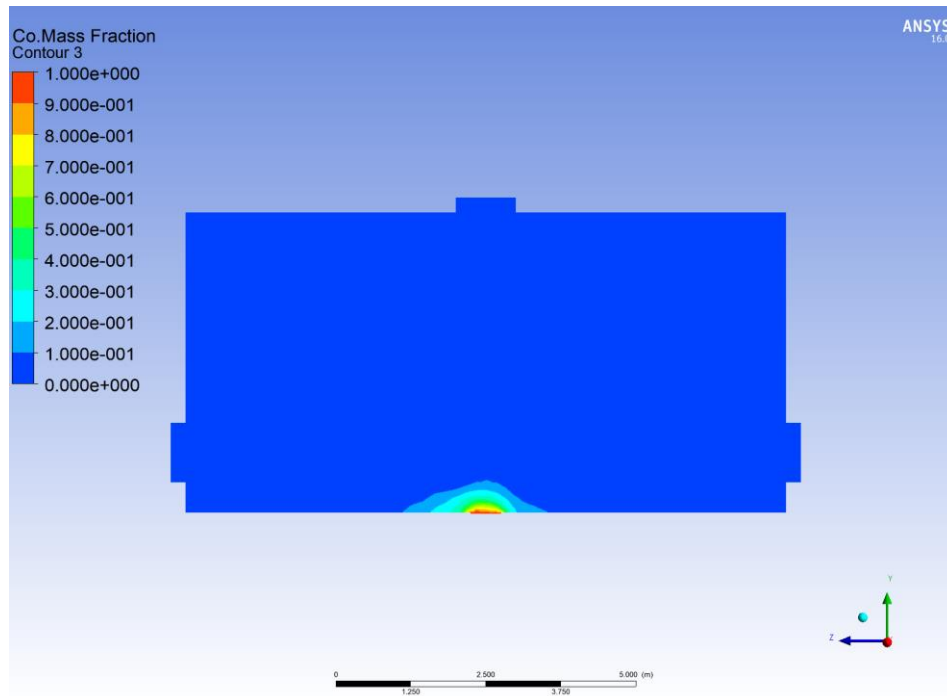


**Figure 36. Carbon monoxide mass fraction contour of scheme 7 (cross section between inlet and outlet)**

## 5. CONCLUSIONS AND FUTURE WORK

### 5.1 Conclusions

A comprehensive comparison between different ventilation installation schemes is conducted in this thesis. Three single-inlet ventilation installation schemes and four different two-inlet models are developed, and the performance and effectiveness of these schemes are compared and examined by CFD simulation. The conclusions of the simulation results are stated below:

- (1) Among three single-inlet ventilation installation schemes, scheme 2 has the best ventilation efficiency. However, single-inlet ventilation system installation schemes have limited effect on the reduction of pollutant concentrations because the high-airflow-velocity area is only concentrated near the cross-sectional area of air inlet and outlet. Ventilation systems have virtually no effect on the area that far from vents. This minimizes the effectiveness of the ventilation system in reducing the concentration of contaminants in confined workplaces.
- (2) Due to the one-to-one correspondence between the air inlet and the air outlet, the single-inlet ventilation system causes the air in confined workplaces to flow from the air inlet to the air outlet in a single direction. Such a ventilation installation scheme causes the concentration of the pollutant to increase at the downwind area which can adversely affect the ventilation effectiveness and threatening the health of workers at downwind area.
- (3) Four two-inlet ventilation system installation schemes significantly increase the ventilation effectiveness of the ventilation system. It allows air to flow more widely

throughout the confined workplace and cover much more volume of space than the conventional method. The contaminant concentration is also controlled within an acceptable level except scheme 4.

- (4) The opposite arrangement of the air inlets can effectively avoid the problem that the air flows in a single direction within the confined workplace so that the pollutant concentration at downwind area can be significantly reduced.
- (5) For recommendation of installation guideline for dilution ventilation system, if the workshop can only accommodate one inlet setting, scheme 2 has the best effectiveness. If two-inlet schemes are allowed, scheme 5 and 7 are the best two schemes to control the contaminant source located at the center of the workshop. If the contaminant source cannot be determined or more overall protection is needed, scheme 6 has the best overall performance among all installation schemes.

## 5.2 Future Work

The thesis is a preliminary attempt to optimize dilution ventilation system installation scheme. Based on the proposed schemes in this thesis, some recommendations for future work are listed as follows:

- (1) This thesis only simulated the most straightforward setting of the industrial workshop which does not have any obstacles in the computational geometry. The obstacles in the workshop can profoundly affect the ventilation performance. A more complex geometry which is more applicable in practice is needed in the future simulation.
- (2) The computational geometry setting of this thesis only focused on small-scale workshop with only one exhaust fan. However, the size of confined workplaces in chemical industry can vary significantly. In many cases, a multi-exhaust ventilation



system needs to be installed in these places. An optimized installation scheme and guideline for a multi-exhaust ventilation system is needed.

- (3) Some ventilation effectiveness evaluation index like contaminant age cannot be predicted in steady-state simulation. Transient simulation is needed in future work to further compare the speed of contaminant removal between different installation schemes.
- (4) This thesis is a qualitative study of the ventilation system which only has simulation results. Experimental data is needed to validate the simulation results since sometimes the simulation results will deviate from the actual situation.

## REFERENCES

1. Crowl, D.A. and J.F. Louvar, *Chemical process safety: fundamentals with applications*. 2nd ed. Prentice Hall international series in the physical and chemical engineering sciences. 2011. xix, 625 pages.
2. ACGIH, *Industrial Ventilation: A Manual of Recommended Practice*. 27th ed. 2010.
3. Boyle, R., *Natural and Artificial Methods of Ventilation*. 1899: Robert Boyle & Son.
4. CENC, *Ventilation for buildings: Design criteria for the indoor environment*. Brussels, European Committee for Standardization, 1998.
5. British Standard Institution., *Indoor environmental input parameters for design and assessment of energy performance of buildings addressing indoor air quality, thermal environment, lighting and acoustics*. 2007: European committee for Standardization.
6. International Organization of Standardization, *Ergonomics of the Thermal Environment: Analytical Determination and Interpretation of Thermal Comfort Using Calculation of the PMV and PPD Indices and Local Thermal Comfort Criteria*. 2005: International Organization for Standardization.
7. Awbi, H.B. *Energy efficient ventilation for retrofit buildings*. in *Proceedings of 48th AiCARR international conference on energy performance of existing buildings*. 2011.
8. Reid, D.B., *Ventilation in American dwellings*. 1858: Wiley & Halsted.
9. Butler, W.F., *Ventilation of buildings*. 1885: D. Van Nostrand.
10. Müller, D., et al., *Mixing Ventilation—Guide on mixing air distribution design, REHVA Guidebook No 19*. Brussels: Federation of European Heating, Ventilation and Air Conditioning Associations. Google Scholar, 2013.

11. Li, Y., M. Sandberg, and L. Fuchs, *Vertical Temperature Profiles in Rooms Ventilated by Displacement: Full-Scale Measurement and Nodal Modelling*. *Indoor Air*, 1992. **2**(4): p. 225-243.
12. Cheong, K., et al., *A study of perceived air quality and sick building syndrome in a field environment chamber served by displacement ventilation system in the tropics*. *Building and environment*, 2006. **41**(11): p. 1530-1539.
13. Xing, H. and H. Awbi, *The neutral height in a room with displacement ventilation*. *Air distribution in rooms: ventilation for health and sustainable environment*, 2000. **2**: p. 783-88.
14. Yu, W., et al., *Thermal effect of temperature gradient in a field environment chamber served by displacement ventilation system in the tropics*. *Building and environment*, 2007. **42**(1): p. 516-524.
15. Tomasi, R., et al., *Experimental evaluation of air distribution in mechanically ventilated residential rooms: Thermal comfort and ventilation effectiveness*. *Energy and Buildings*, 2013. **60**: p. 28-37.
16. Karimipannah, T. and H. Awbi, *Theoretical and experimental investigation of impinging jet ventilation and comparison with wall displacement ventilation*. *Building and Environment*, 2002. **37**(12): p. 1329-1342.
17. Karimipannah, T., et al., *Investigation of air quality, comfort parameters and effectiveness for two floor-level air supply systems in classrooms*. *Building and Environment*, 2007. **42**(2): p. 647-655.
18. Awbi, H.B., *Ventilation systems: design and performance*. 2008: Psychology Press.
19. Awbi, H.B., *Ventilation of buildings*. 2003: Taylor & Francis.

20. Cho, Y., H.B. Awbi, and T. Karimipناه, *Theoretical and experimental investigation of wall confluent jets ventilation and comparison with wall displacement ventilation*. Building and Environment, 2008. **43**(6): p. 1091-1100.
21. Lomas, K.J., *Architectural design of an advanced naturally ventilated building form*. Energy and Buildings, 2007. **39**(2): p. 166-181.
22. Sandberg, M., C. Blomqvist, and M. Sjöberg. *Efficiency of general ventilation systems in residential and office buildings-concepts and measurements*. in *Ventilation*. 1986.
23. Awbi, H.B. and G. Gan. *Evaluation of the overall performance of room air distribution*. in *Proceedings of the 6th International Conference on Indoor Air Quality and Climate, Helsinki*. 1993.
24. Kato, S., *New ventilation efficiency scales based on spatial distribution of contaminant concentration aided by numerical simulation*. ASHRAE transactions, 1988. **94**(2): p. 309-330.
25. Sandberg, M., *What is ventilation efficiency?* Building and environment, 1981. **16**(2): p. 123-135.
26. Sandberg, M. and M. Sjöberg, *The use of moments for assessing air quality in ventilated rooms*. Building and environment, 1983. **18**(4): p. 181-197.
27. Potter, I., *Ventilation effectiveness in mechanical ventilation systems*. 1988: Building Services Research and Information Association.
28. Lim, E., K. Ito, and M. Sandberg, *New ventilation index for evaluating imperfect mixing conditions—Analysis of Net Escape Velocity based on RANS approach*. Building and Environment, 2013. **61**: p. 45-56.

29. Cao, G., et al., *A review of the performance of different ventilation and airflow distribution systems in buildings*. Building and Environment, 2014. **73**: p. 171-186.
30. Davidson, L. and E. Olsson, *Calculation of age and local purging flow rate in rooms*. Building and Environment, 1987. **22**(2): p. 111-127.
31. Melikov, A.K., R. Cermak, and M. Majer, *Personalized ventilation: evaluation of different air terminal devices*. Energy and buildings, 2002. **34**(8): p. 829-836.
32. Melikov, A.K., *Personalized ventilation*. Indoor Air, 2004. **14**(s7): p. 157-167.
33. Nielsen, P.V., *Velocity distribution in a room ventilated by displacement ventilation and wall-mounted air terminal devices*. Energy and Buildings, 2000. **31**(3): p. 179-187.
34. Etheridge, D.W. and M. Sandberg, *Building ventilation: theory and measurement*. Vol. 50. 1996: John Wiley & Sons Chichester, UK.
35. Li, X. and F. Zhu, *Response Coefficient: A New Concept to Evaluate Ventilation Performance with "Pulse" Boundary Conditions*. Indoor and Built Environment, 2009. **18**(3): p. 189-204.
36. Kosonen, R., *The effect of supply air systems on the efficiency of a ventilated ceiling*. Building and environment, 2007. **42**(4): p. 1613-1623.
37. Abel, E., et al., *Achieving the desired indoor climate-energy efficiency aspects of system design*. 2003: Studentlitteratur.
38. Novoselac, A. and J. Srebric, *A critical review on the performance and design of combined cooled ceiling and displacement ventilation systems*. Energy and buildings, 2002. **34**(5): p. 497-509.
39. Olmedo, I., et al., *The risk of airborne cross-infection in a room with vertical low-velocity ventilation*. Indoor air, 2013. **23**(1): p. 62-73.

40. Cao, G., M. Ruponen, and J. Kurnitski, *Experimental investigation of the velocity distribution of the attached plane jet after impingement with the corner in a high room*. Energy and Buildings, 2010. **42**(6): p. 935-944.
41. Macdonald, R.W., R.F. Griffiths, and D.J. Hall, *A comparison of results from scaled field and wind tunnel modelling of dispersion in arrays of obstacles*. Atmospheric Environment, 1998. **32**(22): p. 3845-3862.
42. Jiang, Y., et al., *Natural ventilation in buildings: measurement in a wind tunnel and numerical simulation with large-eddy simulation*. Journal of Wind Engineering and Industrial Aerodynamics, 2003. **91**(3): p. 331-353.
43. Gavelli, F., E. Bullister, and H. Kytomaa, *Application of CFD (Fluent) to LNG spills into geometrically complex environments*. Journal of Hazardous Materials, 2008. **159**(1): p. 158-168.
44. Ronold, A., *Modelling of flow and ventilation within petroleum process plants A2 - Murakami, S*, in *Computational Wind Engineering I*. 1993, Elsevier: Oxford. p. 675-680.
45. Kashi, E., F. Mirzaei, and F. Mirzaei, *Analysis of gas dispersion and ventilation within a comprehensive CAD model of an offshore platform via computational fluid dynamics*. Journal of Loss Prevention in the Process Industries, 2015. **36**: p. 125-133.
46. Freeman, M., R. Spencer, and A. Huber, *Scientific Visualization for Micro-Scale Modeling of Airborne Pollution in Urban Areas*. 2013, EPA.
47. Buckley, R.L., et al., *Modeling Dispersion from Toxic Gas Released after a Train Collision in Graniteville, SC*. Journal of the Air & Waste Management Association, 2007. **57**(3): p. 268-278.

48. Gilfrin, P. and E. Hatfield, *Visualizing Sheffield City Hall Airflow*. AEC Mag., 2005. **23**: p. 25-26.
49. Stern, F., et al., *Verification and validation of CFD simulations*. 1999, IOWA INST OF HYDRAULIC RESEARCH IOWA CITY.
50. Osenbroch, J., B. Hjertager, and T. Solberg, *Computational Fluid Dynamics (CFD) modelling of gas dispersion in offshore modules*", Aalborg University Esbjerg, Niels Bohrs Vej 8, DK-6700, Denmark. CPS 17th Annual International Conference and Workshop on Risk, Reliability and Security, 2002: p. 233-246.
51. Jiang, Y., C. Allocca, and Q. Chen, *Validation of CFD Simulations for Natural Ventilation*. International Journal of Ventilation, 2016. **2**(4): p. 359-369.
52. Hoi, Y., et al., *Validation of CFD Simulations of Cerebral Aneurysms With Implication of Geometric Variations*. Journal of Biomechanical Engineering, 2006. **128**(6): p. 844-851.
53. Li, Y. and A. Delsante, *Natural ventilation induced by combined wind and thermal forces*. Building and Environment, 2001. **36**(1): p. 59-71.
54. Li, Y., et al., *Some examples of solution multiplicity in natural ventilation*. Building and Environment, 2001. **36**(7): p. 851-858.
55. Chen, Z.D. and Y. Li, *Buoyancy-driven displacement natural ventilation in a single-zone building with three-level openings*. Building and Environment, 2002. **37**(3): p. 295-303.
56. Andersen, K.T., *Theory for natural ventilation by thermal buoyancy in one zone with uniform temperature*. Building and Environment, 2003. **38**(11): p. 1281-1289.

57. Andersen, K.T., *Airflow rates by combined natural ventilation with opposing wind—unambiguous solutions for practical use*. Building and Environment, 2007. **42**(2): p. 534-542.
58. Bassiouny, R. and N.S. Koura, *An analytical and numerical study of solar chimney use for room natural ventilation*. Energy and buildings, 2008. **40**(5): p. 865-873.
59. Fitzgerald, S.D. and A.W. Woods, *The influence of stacks on flow patterns and stratification associated with natural ventilation*. Building and Environment, 2008. **43**(10): p. 1719-1733.
60. Mazumdar, S. and Q. Chen, *A one-dimensional analytical model for airborne contaminant transport in airliner cabins*. Indoor air, 2009. **19**(1): p. 3-13.
61. Parker, S., et al. *Contaminant ingress into multizone buildings: an analytical state-space approach*. in *Building Simulation*. 2014. Springer.
62. Nazaroff, W.W., *Inhalation intake fraction of pollutants from episodic indoor emissions*. Building and Environment, 2008. **43**(3): p. 269-277.
63. Wang, H. and Z. Zhai, *Advances in building simulation and computational techniques: A review between 1987 and 2014*. Energy and Buildings, 2016. **128**: p. 319-335.
64. Bastide, A., F. Allard, and H. Boyer, *Natural ventilation-A new method based on the Walton model applied to cross-ventilated buildings having two large external openings*. International Journal of Ventilation, 2007. **6**(3): p. 195-206.
65. Li, Y. and P.V. Nielsen, *CFD and ventilation research*. Indoor Air, 2011. **21**(6): p. 442-453.



66. Norton, T. and D.-W. Sun, *Computational fluid dynamics (CFD)—an effective and efficient design and analysis tool for the food industry: a review*. Trends in Food Science & Technology, 2006. **17**(11): p. 600-620.
67. Norton, T., et al., *Applications of computational fluid dynamics (CFD) in the modelling and design of ventilation systems in the agricultural industry: A review*. Bioresource technology, 2007. **98**(12): p. 2386-2414.
68. Nielsen, P.V., *Fifty years of CFD for room air distribution*. Building and Environment, 2015. **91**: p. 78-90.
69. Kuznik, F., G. Rusaouen, and J. Brau, *Experimental and numerical study of a full scale ventilated enclosure: Comparison of four two equations closure turbulence models*. Building and Environment, 2007. **42**(3): p. 1043-1053.
70. Murakami, S. and A. Mochida, *3-D numerical simulation of airflow around a cubic model by means of the  $k-\epsilon$  model*. Journal of Wind Engineering and Industrial Aerodynamics, 1988. **31**(2-3): p. 283-303.
71. Chen, Q. and W. Xu, *A zero-equation turbulence model for indoor airflow simulation*. Energy and buildings, 1998. **28**(2): p. 137-144.
72. Hasama, T. and S. Kato. *Detached-eddy simulation of wind-induced ventilation to control indoor thermal environments*. in *APS Division of Fluid Dynamics Meeting Abstracts*. 2005.
73. Deevy, M., et al., *Modelling the effect of an occupant on displacement ventilation with computational fluid dynamics*. Energy and Buildings, 2008. **40**(3): p. 255-264.
74. Chen, Q., *Comparison of different  $k-\epsilon$  models for indoor air flow computations*. Numerical Heat Transfer, Part B Fundamentals, 1995. **28**(3): p. 353-369.

75. Zhai, Z.J., et al., *Evaluation of various turbulence models in predicting airflow and turbulence in enclosed environments by CFD: Part 1—Summary of prevalent turbulence models*. Hvac&R Research, 2007. **13**(6): p. 853-870.
76. Zhang, Z., et al., *Evaluation of various turbulence models in predicting airflow and turbulence in enclosed environments by CFD: Part 2—Comparison with experimental data from literature*. Hvac&R Research, 2007. **13**(6): p. 871-886.
77. Wang, H. and Z.J. Zhai, *Analyzing grid independency and numerical viscosity of computational fluid dynamics for indoor environment applications*. Building and environment, 2012. **52**: p. 107-118.
78. Sørensen, D.N. and L.K. Voigt, *Modelling flow and heat transfer around a seated human body by computational fluid dynamics*. Building and environment, 2003. **38**(6): p. 753-762.
79. Bjerg, B., et al., *Modeling of air inlets in CFD prediction of airflow in ventilated animal houses*. Computers and Electronics in Agriculture, 2002. **34**(1-3): p. 223-235.
80. Wang, H. and Z. Zhai, *Application of coarse-grid computational fluid dynamics on indoor environment modeling: Optimizing the trade-off between grid resolution and simulation accuracy*. HVAC&R Research, 2012. **18**(5): p. 915-933.
81. Huang, H. and F. Haghghat, *Modelling of volatile organic compounds emission from dry building materials*. Building and Environment, 2002. **37**(11): p. 1127-1138.
82. Zhao, B., et al., *Particle dispersion and deposition in ventilated rooms: testing and evaluation of different Eulerian and Lagrangian models*. Building and Environment, 2008. **43**(4): p. 388-397.

83. Zhao, B. and P. Guan, *Modeling particle dispersion in personalized ventilated room*. Building and Environment, 2007. **42**(3): p. 1099-1109.
84. Lai, M.K. and A.T. Chan, *Large-eddy simulations on indoor/outdoor air quality relationship in an isolated urban building*. Journal of engineering mechanics, 2007. **133**(8): p. 887-898.
85. Chang, T.-J., H.-M. Kao, and Y.-F. Hsieh, *Numerical study of the effect of ventilation pattern on coarse, fine, and very fine particulate matter removal in partitioned indoor environment*. Journal of the air & waste management association, 2007. **57**(2): p. 179-189.
86. Goodfellow, H.D., *Industrial ventilation design guidebook*. 2001: Elsevier.